

AD\_\_\_\_\_

Award Number: W81XWH-12-1-0467

TITLE: Targeting Nuclear EGFR: Strategies for Improving Cetuximab Therapy in Lung Cancer

PRINCIPAL INVESTIGATOR: Deric L Wheeler

CONTRACTING ORGANIZATION: University of Wisconsin System  
Madison, WI 53715-1218

REPORT DATE: September 2014

TYPE OF REPORT: Annual

PREPARED FOR: U.S. Army Medical Research and Materiel Command  
Fort Detrick, Maryland 21702-5012

DISTRIBUTION STATEMENT: Approved for Public Release;  
Distribution Unlimited

The views, opinions and/or findings contained in this report are those of the author(s) and should not be construed as an official Department of the Army position, policy or decision unless so designated by other documentation.

REPORT DOCUMENTATION PAGE				Form Approved OMB No. 0704-0188	
Public reporting burden for this collection of information is estimated to average 1 hour per response, including the time for reviewing instructions, searching existing data sources, gathering and maintaining the data needed, and completing and reviewing this collection of information. Send comments regarding this burden estimate or any other aspect of this collection of information, including suggestions for reducing this burden to Department of Defense, Washington Headquarters Services, Directorate for Information Operations and Reports (0704-0188), 1215 Jefferson Davis Highway, Suite 1204, Arlington, VA 22202-4302. Respondents should be aware that notwithstanding any other provision of law, no person shall be subject to any penalty for failing to comply with a collection of information if it does not display a currently valid OMB control number. <b>PLEASE DO NOT RETURN YOUR FORM TO THE ABOVE ADDRESS.</b>					
1. REPORT DATE September 2014		2. REPORT TYPE Annual Report		3. DATES COVERED 01 Sep 2013- 31 Aug 2014	
4. TITLE AND SUBTITLE  Targeting Nuclear EGFR: Strategies for Improving Cetuximab Therapy in Luna Cancer				5a. CONTRACT NUMBER	
				5b. GRANT NUMBER W81XWH-12-1-0467	
				5c. PROGRAM ELEMENT NUMBER	
6. AUTHOR(S) Deric L Wheeler, Toni M. Brand, Mari lida  E-Mail: dlwheeler@wisc.edu				5d. PROJECT NUMBER	
				5e. TASK NUMBER	
				5f. WORK UNIT NUMBER	
7. PERFORMING ORGANIZATION NAME(S) AND ADDRESS(ES)  University of Wisconsin System Madison, WI 53715-1218				8. PERFORMING ORGANIZATION REPORT NUMBER	
9. SPONSORING / MONITORING AGENCY NAME(S) AND ADDRESS(ES) U.S. Army Medical Research and Materiel Command Fort Detrick, Maryland 21702-5012				10. SPONSOR/MONITOR'S ACRONYM(S)	
				11. SPONSOR/MONITOR'S REPORT NUMBER(S)	
12. DISTRIBUTION / AVAILABILITY STATEMENT Approved for Public Release; Distribution Unlimited					
13. SUPPLEMENTARY NOTES					
14. ABSTRACT NSCLC is a deadly disease that is driven by a multitude of factors. One of these factors is the epidermal growth factor receptor (EGFR). One of the most prominent molecular targeting agents to the EGFR is the antibody cetuximab. However, most patients develop resistance to this antibody. We have found in models of cetuximab resistance that the EGFR changes its location, to the nucleus, where it is not accessible to the large antibody. Our work over the last several years has discovered how to target the nEGFR, by blocking its translocation to the nucleus through Src Family Kinase blockade. In this first year we have determined 1) that nEGFR can serve as a prognostic factor in early stage NSCLC patients., 2) we have determined that we can target nEGFR in vivo and redistribute to the membrane in vivo, a critical first step for re-sensitizing to cetuximab and 3) developed a new avenue by developing a novel EGFR mutant that lacks its transcriptional potential. This will allow us to directly test the role of nEGFR in biology and cetuximab resistance.					
15. SUBJECT TERMS cetuximab resistance, nuclear EGFR, dasatinib, non-small cell lung cancer					
16. SECURITY CLASSIFICATION OF:			17. LIMITATION OF ABSTRACT  UU	18. NUMBER OF PAGES  39	19a. NAME OF RESPONSIBLE PERSON USAMRMC
a. REPORT U	b. ABSTRACT U	c. THIS PAGE U			19b. TELEPHONE NUMBER (include area code)

## Table of Contents

	<u>Page</u>
<b>Introduction.....</b>	<b>3</b>
<b>Keywords.....</b>	<b>3</b>
<b>Overall Project Summary.....</b>	<b>4</b>
<b>Key Research Accomplishments.....</b>	<b>7</b>
<b>Conclusions.....</b>	<b>7</b>
<b>Publications, Abstracts, Presentations.....</b>	<b>8</b>
<b>Inventions, Patents, Licenses.....</b>	<b>9</b>
<b>Reportable Outcomes.....</b>	<b>9</b>
<b>Other Achievements.....</b>	<b>9</b>
<b>References.....</b>	<b>9</b>
<b>Appendices.....</b>	<b>10</b>

## INTRODUCTION:

The **goals** of this proposal are to **1)** determine if targeting the nuclear EGFR (nEGFR) signaling pathway can increase the efficacy of anti-EGFR antibody based therapies in non-small cell lung cancer (NSCLC) and **2)** determine if nEGFR can serve as a prognostic factor in NSCLC.

The EGFR is a ubiquitously expressed receptor tyrosine kinase (RTK) involved in the etiology of NSCLC. With this, intense efforts have been undertaken to stop EGFR function. These efforts have been highly fruitful as four drugs, including two small tyrosine kinase inhibitors (TKIs, gefitinib and erlotinib) and two antibodies (cetuximab and panitumumab), have moved to the clinic to target EGFR in NSCLC patients. In 2004, the identification of specific genetic mutations within the EGFR kinase domain of adenocarcinomas of the lung that predict response to EGFR-TKIs represented a landmark development in the EGFR field. Unfortunately, no such mutations that predict response to cetuximab have yet been identified. Clinical trials (FLEX trial<sup>1</sup>) investigating cetuximab in NSCLC showed clinical benefit. However, not all patients respond to cetuximab therapy and most acquire resistance to cetuximab.

It is well established that the EGFR can rely on two distinct compartments of signaling: **1)** Classical membrane bound signaling (classical EGFR pathway)<sup>2</sup> and **2)** nuclear signaling (nEGFR pathway)<sup>3</sup>. In the nEGFR pathway, recent data suggests that **the EGFR is phosphorylated by Src family kinases (SFKs)<sup>4,5</sup> and AKT<sup>6</sup>, which are necessary, early, events for trafficking EGFR from the membrane to the nucleus.** In the nucleus EGFR is able to promote the transcription of genes essential for cell proliferation and cell cycle regulation<sup>6-12</sup>.

To explore molecular mechanisms of resistance to cetuximab in NSCLC our lab developed a series of cetuximab-resistant models using NSCLC cancer lines<sup>13</sup>. During investigations into potential molecular mechanisms of resistance we found that NSCLC tumor cells that acquired resistance to cetuximab had increased SFK activity<sup>14</sup> and increased nEGFR<sup>5</sup>. Further investigation revealed that SFKs regulate EGFR translocation to the nucleus<sup>5</sup> and the nuclear activity of EGFR contributes to resistance to cetuximab therapy<sup>5</sup>. However, this preliminary work has led to several questions that form the **focus** of this application: **1)** Can blocking SFK and AKT activity decrease nuclear translocation of the EGFR *in vivo*, **2)** will this lead to increased expression of EGFR on the cell membrane, **3)** will this increase sensitivity to cetuximab therapy and **4)** what is the prevalence of nEGFR in NSCLC patient biopsies and can it serve as a prognostic factor? In this proposal we **hypothesize** that nEGFR contributes to NSCLC resistance to cetuximab and that targeting nEGFR, by abrogating its translocation to the nucleus via SFK or AKT inhibition, followed by targeting membrane bound EGFR with cetuximab will increase therapeutic response of NSCLC tumors to cetuximab. To test this hypothesis we propose the following specific aims:

**Specific Aim 1:** To determine if SFK or AKT inhibition can 1) block EGFR translocation to the nucleus 2) decrease nEGFR function and 3) increase EGFR expression on the cell membrane.

**Specific Aim 2:** Determine if targeting nEGFR, via SFK or AKT inhibition, can increase therapeutic response of nEGFR positive, cetuximab-resistant NSCLC tumors to cetuximab.

**Specific Aim 3:** Determine the prevalence of nEGFR protein expression in NSCLC using IHC and AQUA/Vectra analyses and determine if it serves as a prognostic factor in NSCLC.

**KEYWORDS:** cetuximab, epidermal growth factor receptor, src family kinases, non-small cell lung cancer, resistance, therapy, dasatinib, nuclear, Axl, receptor tyrosine kinase

## OVERALL PROJECT SUMMARY:

In the second year of this DoD-LCRP award we have focused on two areas of the SOW; the first being in Aim 1 and the second being expansion of Aim 3 as described below:

**Specific Aim 1:** To determine if SFK or AKT inhibition can 1) block EGFR translocation to the nucleus and if this leads to decreased nEGFR function and 2) increase EGFR expression on the cell membrane. Over the last year we have made several findings in molecular signaling that leads to nuclear translocation of the EGFR. These are highlighted briefly below.

*Nuclear translocation of EGFR is linked to the Axl Receptor tyrosine kinase:* One of the major goals of our laboratory is to modulate EGFR trafficking to the nucleus to increase therapeutic response to cetuximab. In studies over the last year we have learned that the receptor tyrosine kinase Axl is critical for nuclear EGFR translocation. In a paper recently submitted to *Oncogene* we reported that Axl and EGFR bind, Axl phosphorylates EGFR resulting in binding of Src Family Kinases, which in turn phosphorylate tyrosine 1101, the site necessary for nuclear translocation of the EGFR. By targeting Axl with siRNA or degrading antibodies we could completely prevent nuclear translocation of the EGFR. This suggests that targeting Axl, rather than the Src Family Kinases, may represent a novel approach to blocking EGFR nuclear translocation; the major goal of this grant.

*AKT inhibition does not result in robust blockade of EGFR nuclear translocation:* It has been reported that targeting AKT may be able to block EGFR nuclear translocation. However, studies *in vivo* looking at nuclear versus membrane EGFR after AKT blockade did not show a robust response prevention of nuclear EGFR. This suggests that targeting Src Family Kinases, rather than AKT, may be the best opportunity to therapeutically intervene.

*Cetuximab resistance is mediated by kinase independent functions of the EGFR:*

In 2009 we published data that indicated that overexpression of EGFR-WT-NLS resulted in increased cetuximab resistance in *in vitro* and *in vivo* models, however, what functions of nEGFR that mediate this resistance could not be determined via the use of this fusion protein. To elucidate what functions of nEGFR mediate this resistant phenotype we have taken several approaches (**Figure 1**). Firstly, we transiently expressed 1) EGFR-WT-NLS and 2) EGFR-KD-NLS in the LSCC and HNSCC cetuximab-sensitive parental control cells HP and SP, where we found that both fusion proteins were effectively nuclear localized to similar degrees (**Figure 1A**). Next, cells expressing each construct were plated and challenged with cetuximab for 72 hours (**Figure 1B**). The results indicated that, relative to vector controls, both EGFR-WT-NLS and EGFR-KD-NLS expressing cells became resistant to cetuximab therapy (**Figure 1B**). In a second, independent approach, we cloned a C-terminal domain (CTD) truncation variant of the EGFR, where the N-terminus, transmembrane domain, and kinase domain were deleted (**Figure 1C**). We hypothesized that this EGFR variant (EGFR-CTD-NLS), lacking its ability to be localized on the plasma membrane and function as a kinase, could still translocate to the nucleus and function as a co-transcription factor. This approach was based off our previous success investigating HER3 co-transcriptional activities through the use of a HER3-CTD construct that was transcriptionally viable<sup>15,16</sup>. The results from this experimentation indicated that, relative to vector controls, EGFR-CTD-NLS could also lead to increased cetuximab resistance, similar to the findings for the full length EGFR-WT-NLS (**Figure 1D**). Collectively these data strongly indicate that nEGFR, independent of its kinase activities, can drive resistance

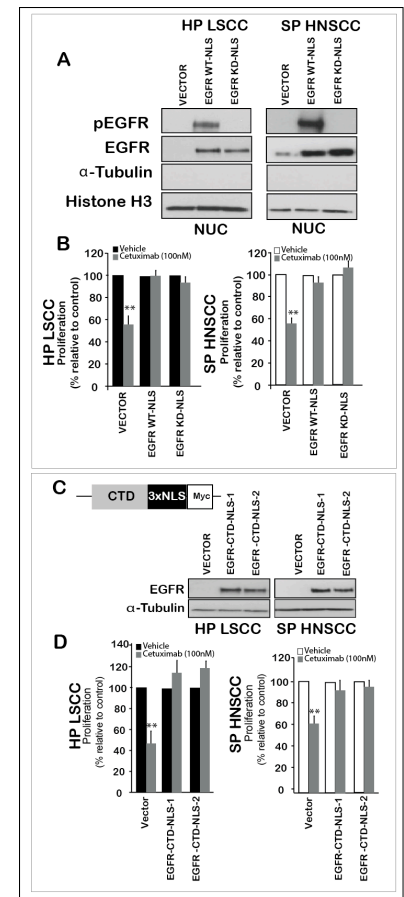


**Figure 1: Nuclear EGFR, independent of its kinase activity, can drive cetuximab resistance.** A) LSCC (HP) and HNSCC (SP) parental lines were transfected with EGFRWT-NLS or EGFR-KD-NLS. B) Both EGFRWT-NLS or EGFRKD-NLS could confer resistance to cetuximab upon cetuximab challenge. C&D) Isolation of the C-terminal of the EGFR could confer resistance to cetuximab therapy. \*\* P<0.005

to cetuximab therapy providing further rationale for the investigation of nEGFR kinase independent functions in cetuximab resistance.

**De Novo derived, cetuximab resistant tumors have increased nuclear EGFR:** One criticism we often receive is

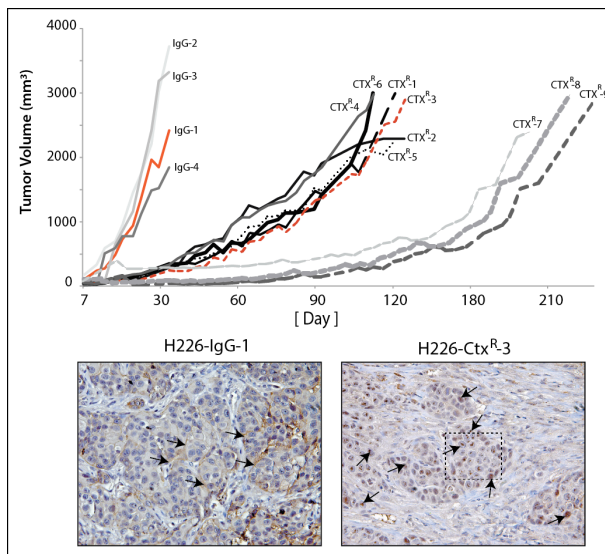


**Figure 2: Cetuximab resistant tumors derived *in vivo* harbor increased nEGFR as compared to IgG control tumors.** Arrows depict LSCC nuclear foci. H226 was used with similar results seen in HNSCC1 and 6 (data not shown).

that our model of cetuximab resistance was developed *in vitro* and it is not clear whether nuclear EGFR would be present in resistant tumors developed *in vivo*. To mimic the development of acquired resistance to cetuximab in the clinical setting we have previously developed numerous *de novo* acquired resistant models *in vivo* by treating established cetuximab sensitive tumors with continued cetuximab therapy until resistant tumor emerge<sup>17</sup>. As depicted in **Figure 2**, tumors treated with IgG grew rapidly, while tumors treated with cetuximab displayed initial growth control. Acquired resistance was observed at approximately 30-60 days in 65% of tumors, where there was marked tumor growth in the presence of continued cetuximab therapy. IHC Analysis of these tumors indicated that 7/9 had increased nEGFR expression as compared to IgG treated tumors (**Figure 2**). This work has been replicated in other SCC models including *de novo* tumors established from the cetuximab sensitive cell lines H292 and SCC1.

**Chemically induced lung tumors have increased nuclear EGFR:** To make more robust models of lung cancers harboring nuclear EGFR we created chemically derived tumors using NTCU as previously described. This tumor model will be used in Aim 2 for functional targeting studies of EGFR. Briefly, we started a collaboration with Dr. Ming You (MCW Cancer Center Director and consultant) who was the first to use NTCU to generate SCC in the mouse lung<sup>18</sup>. He determined that FVB/N mice gave approximately four SCC lesions/mouse eight months after treatment with NTCU. Further, the histopathology of the mouse lung SCC is similar to that seen in humans with well-defined pathological development from bronchial hyperplasia to SCC. To determine if chemically derived LSCC tumors in mice harbor nEGFR we stained 20 independent tumors and analyzed for nEGFR expression (**Figure 3B**). Strikingly, the results showed that like human (**Figure 3A**), mouse LSCC harbored nEGFR whereas normal tissue had no nEGFR expression. Finally, of note, cetuximab does not react with the mouse EGFR. To overcome this experimental problem we have obtained an MTA from ImClone that has generated a murine anti-EGFR antibody, termed ME1. This antibody binds the murine EGFR and inhibits its activity<sup>19</sup>.

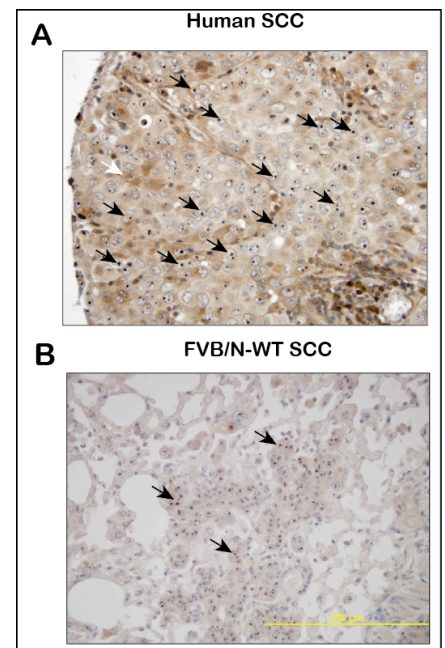


**Figure 3: NTCU derived LSCC tumors harbor nEGFR.** A) Human LSCC stained for nEGFR. B) Mouse NTCU treated LSCC tumor harbor nEGFR.

**Specific Aim 2:** Determine if targeting nEGFR, via SFK or AKT inhibition, can increase therapeutic response of nEGFR positive, cetuximab-resistant NSCLC tumors to cetuximab. In specific Aim 1 we originally aimed to use cells that developed acquired resistance to cetuximab therapy *in vitro*. However we have determined that *de novo* and chemically derived tumors have increased nuclear EGFR and that these models may increase the robustness of targeting nuclear EGFR in Aim 2. This will serve as the final focus of our work in year 3 of this grant.

**Specific Aim 3:** Determine the prevalence of nEGFR protein expression in NSCLC using IHC and AQUA analyses and determine if it serves as a prognostic factor in NSCLC. The focus of this aim was to use two

NSCLC TMAs with various stages of NSCLC. In a first effort we focused our time on the 88 patient TMA that contained only stage I and II patients. The findings from this study have been reported last year and published. We have expanded on this and turned our attention to determining if nuclear EGFR could serve as a predictive factor for cetuximab response in LSCC.

**This was written as an aim in our recent R01 application and is placed here for completeness of design.**

*Determine if nEGFR expression is a predictive biomarker for cetuximab resistance in advanced LSCC.* To accomplish this aim we will determine nEGFR levels in human LSCC tumor specimens and test for a correlation with cetuximab clinical benefit. We will examine nEGFR expression in human tumor specimens (tissue microarray) obtained from the University of Chicago iBridge Network.

**Hypothesis** – We hypothesize that the clinical benefit of cetuximab in advanced LSCC patients will be predicted by nEGFR expression.

**Rationale** – Randomized trials have documented that the addition of cetuximab to conventional chemotherapy in advanced NSCLC results in minimal improvements in clinical outcome<sup>20</sup>. We and others have hypothesized that the marginal benefit observed is a consequence of inadequate patient selection; a robust predictive biomarker for cetuximab efficacy in NSCLC has not been identified<sup>21,22</sup>. Total EGFR expression has been correlated with cetuximab survival benefit, however, the predictive power is quite modest<sup>23</sup>. We have recently shown that nEGFR is a prognostic factor in early stage NSCLC<sup>24</sup>. Further, in experimental model systems, we have shown that elevated nEGFR leads to cetuximab resistance in a variety of cancers<sup>5,14,25-27</sup>. Therefore, it is biologically plausible that nEGFR may be a predictive biomarker of cetuximab efficacy and permit optimal patient selection for cetuximab use in advanced NSCLC.

**Clinical Sample Set** – We will confirm the prognostic significance of nEGFR in advanced LSCC (stage IV) and determine if nEGFR is a predictive biomarker for cetuximab efficacy. In order to do so, we will employ the thoracic oncology research program standard operating procedure (SOP) within the iBridge network (<http://www.ibridgenetwork.org>) directed by Dr. Salgia (collaborator) at the University of Chicago. The iBridge network SOP is a large research bioinformatics platform representing more than 4000 total lung cancer samples and tissue microarrays. Specimens are linked to comprehensive clinical information including outcomes (RR, OS, PFS) as well as characteristics such as age, sex, race, stage at initial diagnosis, and therapeutic history. The dataset has contributed to several large-scale lung cancer analyses similar to the analysis proposed herein<sup>28,29</sup>. Among regional utilizers/contributors to the iBridge network, cetuximab was frequently employed in the advanced NSCLC population prior to the availability of phase III trial evidence of minimal clinical benefit. Consequently, we have identified 200 advanced LSCC patients treated with carboplatin/paclitaxel/cetuximab. An additional 300 advanced LSCC patients treated with carboplatin/paclitaxel have been identified. To extrapolate from the Lynch trial, there was no difference in overall survival between chemotherapy with or without cetuximab<sup>30</sup>. However, our hypothesis is that the predictive value of cetuximab response would be dependent on nuclear or non-nuclear localization of EGFR. As can be appreciated, the iBridge network has the SOP of our database as well as the tumor tissue repository. This was initially created by Dr. Salgia and his colleagues with ARRA funding and has been made available to anyone for free. Since establishment, the initial SOP has been licensed by over 80 institutions (including Harvard, Hopkins, Yale, Boston University, Columbia, etc). The SOP is available in Microsoft Access, Oracle based system, as well as RedCap. In the metropolitan Chicago area, we have a combined effort with Rush, UIC, North Shore, Ingalls Hospital, and our phase II consortium (containing 13 affiliates).

*Correlation of EGFR localization and clinical outcome* – Tissue microarrays will be prepared from this patient cohort through the University of Chicago Pathology Core. We will then stain, using several EGFR antibodies that have been used in analysis of nEGFR<sup>24</sup>. In particular, we will determine the expression of cytoplasmic/membranous versus nEGFR and correlate with clinical benefit rate. **Expected results** – We expect that nEGFR expression will be prognostic in advanced LSCC patients with lower clinical benefit rates with both chemotherapy and the combination of chemotherapy and cetuximab in nEGFR expressors compared to nEGFR non-expressors. Critically, we expect that nEGFR expression will be associated with no improvement in clinical



benefit rate with the addition of cetuximab. In contrast, we anticipate that advanced LSCC patients without nEGFR expression will significantly benefit from the addition of cetuximab.

**Statistical analysis** – Power analysis is based on clinical benefit rate, defined by the rate of response plus stable disease at 12 weeks. The four groups for comparison are (1) nEGFR negative treated with chemotherapy (CT), (2) nEGFR negative treated with cetuximab and chemotherapy (CTX+CT), (3) nEGFR positive treated with CT and (4) nEGFR positive treated with CTX + CT. Based on our preliminary work, we expect 40% or more samples to be nEGFR negative in this advanced stage population. The clinical benefit rates of both CT and CTX+CT are expected to be about 30% for nEGFR positive groups (i.e. there will be no benefit to the addition of CTX). The clinical benefit rate from CT is estimated to be higher in the nEGFR negative group by about 5%-10% (prognostic). We hypothesize the clinical benefit rate will be higher with the addition of CTX in the nEGFR negative cohort (predictive). For statistical analysis, we estimate the absolute magnitude of the CTX benefit in the nEGFR negative cohort to be approximately 20%. We perform our power analysis based on detecting this predictive effect of nEGFR status using an interaction logistic regression model, which is to detect statistically significant interaction between nEGFR status and cetuximab. The type I error is set at 10% level and the resulting powers range from 0.78 or 0.92 depending on the possible values for the proportion of nEGFR negative, clinical benefit rates of CT in nEGFR negative and positive groups (see Tables XX and XX in the appendix). The calculation is based on 200 samples of CT+CTX and 300 samples of CT alone. We will conduct our analysis based on logistic regression models.

**Potential Pitfalls and Alternative Approaches** – Our laboratory reported that nEGFR leads to resistance to cetuximab therapy. However, which nuclear function of EGFR that plays a role in this process is not yet known. To investigate this, we developed a nEGFR mutant that lacks the ability to mediate transcription. This results in a potential pitfall in Aim 2A, since tumors lacking nEGFR transcriptional functions may grow differently from tumors overexpressing EGFRWT. In order to determine cetuximab response we will do both time-matched and size-matched cetuximab response experiments and measure the tumor growth delay as compared to the EGFRWT control. Due to the heterogeneity of the studied patient population, clinical outcomes (RR, OS, PFS) will vary. This potential pitfall is limited by design with inclusion of only metastatic patients. If statistical significance is compromised by patient heterogeneity in Aim 2B, a number of approaches may be taken to increase power and elucidate the predictive value of nEGFR expression including time-to-event analysis. Additional tissue samples are available from the University of Wisconsin if analyses are underpowered (see Traynor letter). Moreover, analysis of nEGFR expression as a continuous variable and/or examination of the cytoplasmic-to-nEGFR ratio may provide opportunities to enhance statistical power of correlations between EGFR expression and localization with clinical outcomes.

## **KEY RESEARCH ACCOMPLISHMENTS:**

- Axl receptor tyrosine kinase is implicated in EGFR nuclear trafficking
- EGFR can mediate cetuximab resistance independent of its kinase activity
- Chemically derived tumors harbor nuclear EGFR
- *De novo* derived cetuximab resistant tumors harbor nuclear EGFR
- AKT inhibition is not robust in preventing nuclear EGFR trafficking

## **CONCLUSIONS:**

NSCLC is a deadly disease that is driven by a multitude of factors. One of these factors is the epidermal growth factor receptor (EGFR). One of the most prominent molecular targeting agents to the EGFR is the antibody cetuximab. However, most patients develop resistance to this antibody. We have found in models of cetuximab resistance that the EGFR changes its location, to the nucleus, where it is not accessible to the large antibody. Our work over the last several years has discovered how to target the nEGFR, by blocking its translocation to the nucleus through Src Family Kinase blockade.

In the **First year** we have determined that nEGFR can serve as a prognostic factor in early stage NSCLC



patients. We are building on this finding to see if nEGFR can serve as a prognostic factor for late stage patients, a goal of Aim 3. Secondly we have determined that we can target nEGFR in vivo and redistribute to the membrane in vivo, a critical first step for re-sensitizing to cetuximab. Finally, we have developed a new avenue by developing a novel EGFR mutant that lacks its transcriptional potential. This will allow us to directly test the role of nEGFR in biology and cetuximab resistance.

In the **Second year** we have determined several key findings. The first is that Axl receptor tyrosine kinase is a critical mediator of nuclear translocation of the EGFR. This novel finding may indicate that target Axl may serve as a secondary approach to block the nuclear functions of EGFR. Secondly we found that tumors that develop resistance in vivo have nuclear EGFR and further, chemically derived tumors harbor nuclear EGFR. Thirdly, we have found that targeting nuclear EGFR by blocking the AKT pathway had minimal effects as compared to blocking the Src Family Kinases. Further investigations will focus on SFK blockade as well as targeting Axl.

## **PUBLICATIONS, ABSTRACTS AND PRESENTATIONS**

### *Lay Press, Highlight features*

FY14 LCRP publicity materials; LC110082 - Targeting Nuclear EGFR: Strategies for Improving Cetuximab Therapy in Lung Cancer) was highlighted in our upcoming FY14 LCRP publicity materials.

### *Publications*

1. Li, C, Brand, TM Iida, M, Huang, S, Armstrong, EA, Van Der Kogel, B, **Wheeler, DL**. Human epidermal growth factor receptor 3 (HER3) blockade with U3-1287/AMG888 enhances the efficacy of radiation therapy in lung and head and neck carcinomas, *Discov. Med.* 2013 Sep;16(87):79-92. PMID: 23998444, PMCID: PMC3901945
2. Iida, M, Brand TM, Starr, M, **Wheeler, DL**, The EGFR blocking antibodies, SYM004, can overcome acquired resistance to cetuximab, *Neoplasia* 2013 Oct;15(10):1196-206. PMID:24204198, PMCID:PMC3819635
3. Rolle, CE, Surati, M, Nandi, S, Kanteti, R, Yala, S, Tretiakova, M, Arif, Q, Hembrough, T, Brandon, TM, **Wheeler, DL**, Husain, AN, Vokes, EE, Bharati, A, Salgia, R. MET inhibition and Topoisomerase I inhibition synergize to block cell growth of small cell lung cancer. *Mol Cancer Ther.* 2013 Dec 10. PMID:24327519, PMCID: in process
4. Stegeman, Span, Kaanders, JHAM, H, Kaanders, Verhheijen, MM, Peeters, WJ, **Wheeler, DL**, Iida, M, Grenman, R, Van der Kogel, AJ, Span, PN, and Bussink, J. Combining radiotherapy with MEK1/2, STAT5 or STAT6 inhibition reduces survival of head and neck cancer lines, *Mol. Cancer*, 2013 Nov 5;12(1):133. PMID:24192080, PMCID:PMC3842630
5. Brand, TM, Iida, M, Dunn, E, Luthar, N, Kostopoulus, KT, Corrigan, KL, Yang, Wleklinski, D, Wisinski, KB, Salgia, R, **Wheeler, DL**. Nuclear EGFR serves as a functional molecular target in Triple-negative breast cancer *Mol Cancer Ther.* 2014 May;13(5):1356-68. PMID: 24634415, PMCID: PMC4013210
6. Brand, TM, Iida, M, Stein, AP, Corrigan, KL, Braverman, CM, Luthar, N, Toulany, M, Gill, PS, Salgia, R, Kimple, RJ, **Wheeler, DL**. AXL Mediates Resistance to Cetuximab Therapy. *Cancer research* (2014). PMID: 25136066, PMCID:Pending
7. Iida, M, Brand TM, Starr, M, Huppert, E, Corrigan, K, Salgia, R, **Wheeler, DL**, Overcoming acquired resistance to cetuximab by blockade of HER3 using U3-1287. (*Molecular Cancer*, Accepted)

8. Brand, TM, Iida, M, E, Corrigan, K, Salgia, R, **Wheeler, DL**, Axl is necessary for nuclear translocation of the EGFR in tumors with acquired resistance. (Oncogene, submitted)

### *Abstracts*

1. Villaflor, VM, Wheeler, DL, Iida, M, Vidwans, S, Turski, M, Brand TM, Won, B, Ferguson, M, Patti, M, Posner, M, Waxman, I, Vokes, EE, Salgia, R, Genetic alterations in Esophageal Cancers—Detection by next generation sequencing and potential for therapeutic targets. ASCO, 2014
2. Brand, TM, Iida, M, Corrigan, KL, Luthar, N, Hornung, M, Toulany, Gill, P, Salgia, R, **Wheeler, DL**, The receptor tyrosine kinase Axl plays a role in acquired resistance to cetuximab. Am. Assoc. Cancer Res. San Diego, CA, April 2014. **Late-Breaking Abstract**

### *Invited reviews*

1. Brand, TM, Iida, M, Luthar, N, Starr, MM, Huppert, EJ, **Wheeler, DL**. Nuclear EGFR as a molecular target in cancer. *Radiother Oncol*. 2013 Sep;108(3):370-7. PMID: 23830194, PMCID: PMC3818450

### **INVENTIONS, PATENTS, LICENSE; N/A**

### **REPORTABLE OUTCOMES:**

- Licenses applied for and/or issued N/A
- Degrees obtained that are supported by this award; N/A/
- Development of cell lines, tissue or serum repositories; N/A
- informatics such as databases and animal models, etc.; N/A
- Employment or research opportunities applied for and/or received based on experience/training supported by this award N/A
- 

### **OTHER ACHIEVEMENTS:**

- Promoted to Associate Professor with tenure at the University of Wisconsin School Of Medicine and Public Health.
- Graduate Student Toni M. Brand received her PhD in Molecular and Cellular Pathology.
- Submitted an R01 expanding nuclear EGFR and cetuximab resistance; R01 grant scored a 23 percentile, has been responded to and resubmitted and is currently under review in October 2014.
- Submitting an R01 application to the NIH on the role of Axl in resistance to cetuximab therapy in February 2015.

### **REFERENCES**

1. Pirker, R., *et al*. Cetuximab plus chemotherapy in patients with advanced non-small-cell lung cancer (FLEX): an open-label randomised phase III trial. *Lancet* **373**, 1525-1531 (2009).
2. Yarden, Y. & Sliwkowski, M.X. Untangling the ErbB signalling network. *Nat Rev Mol Cell Biol* **2**, 127-137 (2001).
3. Wang, S.C. & Hung, M.C. Nuclear translocation of the epidermal growth factor receptor family membrane tyrosine kinase receptors. *Clinical cancer research : an official journal of the American Association for Cancer Research* **15**, 6484-6489 (2009).
4. Li, C., Iida, M., Dunn, E.F. & Wheeler, D.L. Dasatinib blocks cetuximab- and radiation-induced nuclear translocation of the epidermal growth factor receptor in head and neck squamous cell carcinoma. *Radiother Oncol* (2010).

5. Li, C., Iida, M., Dunn, E.F., Ghia, A.J. & Wheeler, D.L. Nuclear EGFR contributes to acquired resistance to cetuximab. *Oncogene* **28**, 3801-3813 (2009).
6. Huang, W.C., *et al.* Nuclear Translocation of Epidermal Growth Factor Receptor by Akt-dependent Phosphorylation Enhances Breast Cancer-resistant Protein Expression in Gefitinib-resistant Cells. *The Journal of biological chemistry* **286**, 20558-20568 (2011).
7. Lin, S.Y., *et al.* Nuclear localization of EGF receptor and its potential new role as a transcription factor. *Nat Cell Biol* **3**, 802-808 (2001).
8. Lo, H.W., *et al.* Nuclear interaction of EGFR and STAT3 in the activation of the iNOS/NO pathway. *Cancer Cell* **7**, 575-589 (2005).
9. Hanada, N., *et al.* Co-regulation of B-Myb expression by E2F1 and EGF receptor. *Mol Carcinog* **45**, 10-17 (2006).
10. Jaganathan, S., *et al.* A functional nuclear epidermal growth factor receptor, SRC and stat3 heteromeric complex in pancreatic cancer cells. *PloS one* **6**, e19605 (2011).
11. Hung, L.Y., *et al.* Nuclear epidermal growth factor receptor (EGFR) interacts with signal transducer and activator of transcription 5 (STAT5) in activating Aurora-A gene expression. *Nucleic Acids Res* **36**, 4337-4351 (2008).
12. Lo, H.W., Cao, X., Zhu, H. & Ali-Osman, F. Cyclooxygenase-2 is a novel transcriptional target of the nuclear EGFR-STAT3 and EGFRvIII-STAT3 signaling axes. *Molecular cancer research : MCR* **8**, 232-245 (2010).
13. Wheeler, D.L., *et al.* Mechanisms of acquired resistance to cetuximab: role of HER (ErbB) family members. *Oncogene* **27**, 3944-3956 (2008).
14. Wheeler, D.L., *et al.* Epidermal growth factor receptor cooperates with Src family kinases in acquired resistance to cetuximab. *Cancer biology & therapy* **8**, 696-703 (2009).
15. Brand, T.M., *et al.* Mapping C-Terminal Transactivation Domains of the Nuclear HER Family Receptor Tyrosine Kinase HER3. *PLoS One* **8**, e71518 (2013).
16. Brand, T.M., Iida, M., Luthar, N. & Wheeler, D.L. Mapping the transcriptional activation domains of the HER family of receptor tyrosine kinases. in *American Association of Cancer Research* (Washington, DC, 2013).
17. Iida, M., *et al.* Sym004, a novel EGFR antibody mixture, can overcome acquired resistance to cetuximab. *Neoplasia* **15**, 1196-1206 (2013).
18. Wang, Y., *et al.* A chemically induced model for squamous cell carcinoma of the lung in mice: histopathology and strain susceptibility. *Cancer research* **64**, 1647-1654 (2004).
19. Surguladze, D., *et al.* Tumor necrosis factor-alpha and interleukin-1 antagonists alleviate inflammatory skin changes associated with epidermal growth factor receptor antibody therapy in mice. *Cancer research* **69**, 5643-5647 (2009).
20. Pujol, J.L., *et al.* Meta-analysis of individual patient data from randomized trials of chemotherapy plus cetuximab as first-line treatment for advanced non-small cell lung cancer. *Lung cancer* **83**, 211-218 (2014).
21. Di Maio, M. Is there still room for large registrative trials in unselected cancer patients? The case of anti-epidermal growth factor receptor antibodies in advanced non-small-cell lung cancer. *Expert Opin. Biol. Ther.* **11**, 1131-1133 (2011).
22. Khambata-Ford, S., *et al.* Analysis of potential predictive markers of cetuximab benefit in BMS099, a phase III study of cetuximab and first-line taxane/carboplatin in advanced non-small-cell lung cancer. *Journal of clinical oncology : official journal of the American Society of Clinical Oncology* **28**, 918-927 (2010).
23. Pirker, R., *et al.* EGFR expression as a predictor of survival for first-line chemotherapy plus cetuximab in patients with advanced non-small-cell lung cancer: analysis of data from the phase 3 FLEX study. *The lancet oncology* **13**, 33-42 (2012).
24. Traynor, A.M., *et al.* Nuclear EGFR protein expression predicts poor survival in early stage non-small cell lung cancer. *Lung cancer* **81**, 138-141 (2013).
25. Brand, T.M., *et al.* Nuclear Epidermal Growth Factor Receptor Is a Functional Molecular Target in Triple-Negative Breast Cancer. *Molecular cancer therapeutics* (2014).

26. Iida, M., Brand, T.M., Campbell, D.A., Li, C. & Wheeler, D.L. Yes and Lyn play a role in nuclear translocation of the epidermal growth factor receptor. *Oncogene* **32**, 759-767 (2013).
27. Li, C., Iida, M., Dunn, E.F. & Wheeler, D.L. Dasatinib blocks cetuximab- and radiation-induced nuclear translocation of the epidermal growth factor receptor in head and neck squamous cell carcinoma. *Radiotherapy and oncology : journal of the European Society for Therapeutic Radiology and Oncology* **97**, 330-337 (2010).
28. Carey, G.B., *et al.* Utilisation of a thoracic oncology database to capture radiological and pathological images for evaluation of response to chemotherapy in patients with malignant pleural mesothelioma. *BMJ open* **2**(2012).
29. Surati, M., *et al.* Proteomic characterization of non-small cell lung cancer in a comprehensive translational thoracic oncology database. *Journal of clinical bioinformatics* **1**, 1-11 (2011).
30. Lynch, T.J., *et al.* Cetuximab and first-line taxane/carboplatin chemotherapy in advanced non-small-cell lung cancer: results of the randomized multicenter phase III trial BMS099. *Journal of clinical oncology : official journal of the American Society of Clinical Oncology* **28**, 911-917 (2010).

## APPENDICES:

Papers in part supported by this grant:

Brand, T.M., *et al.* AXL Mediates Resistance to Cetuximab Therapy. *Cancer research* (2014).

Brand, T.M., *et al.* Nuclear epidermal growth factor receptor is a functional molecular target in triple-negative breast cancer. *Molecular cancer therapeutics* **13**, 1356-1368 (2014).

## Nuclear Epidermal Growth Factor Receptor Is a Functional Molecular Target in Triple-Negative Breast Cancer

Toni M. Brand<sup>1</sup>, Mari Iida<sup>1</sup>, Emily F. Dunn<sup>1</sup>, Neha Luthar<sup>1</sup>, Kellie T. Kostopoulos<sup>1</sup>, Kelsey L. Corrigan<sup>1</sup>, Matthew J. Wlekinski<sup>1</sup>, David Yang<sup>2</sup>, Kari B. Wisinski<sup>3</sup>, Ravi Salgia<sup>4</sup>, and Deric L. Wheeler<sup>1</sup>

### Abstract

Triple-negative breast cancer (TNBC) is a subclass of breast cancers (i.e., estrogen receptor-negative, progesterone receptor-negative, and HER2-negative) that have poor prognosis and very few identified molecular targets. Strikingly, a high percentage of TNBCs overexpresses the EGF receptor (EGFR), yet EGFR inhibition has yielded little clinical benefit. Over the last decade, advances in EGFR biology have established that EGFR functions in two distinct signaling pathways: (i) classical membrane-bound signaling and (ii) nuclear signaling. Previous studies have demonstrated that nuclear EGFR (nEGFR) can enhance resistance to anti-EGFR therapies and is correlated with poor overall survival in breast cancer. On the basis of these findings, we hypothesized that nEGFR may promote intrinsic resistance to cetuximab in TNBC. To examine this question, a battery of TNBC cell lines and human tumors were screened and found to express nEGFR. Knockdown of EGFR expression demonstrated that TNBC cell lines retained dependency on EGFR for proliferation, yet all cell lines were resistant to cetuximab. Furthermore, Src Family Kinases (SFKs) influenced nEGFR translocation in TNBC cell lines and *in vivo* tumor models, where inhibition of SFK activity led to potent reductions in nEGFR expression. Inhibition of nEGFR translocation led to a subsequent accumulation of EGFR on the plasma membrane, which greatly enhanced sensitivity of TNBC cells to cetuximab. Collectively, these data suggest that targeting both the nEGFR signaling pathway, through the inhibition of its nuclear transport, and the classical EGFR signaling pathway with cetuximab may be a viable approach for the treatment of patients with TNBC. *Mol Cancer Ther*; 13(5); 1356–68. ©2014 AACR.

### Introduction

Approximately 15% to 20% of all breast cancers lack expression of the estrogen receptor, progesterone receptor, and HER2, and are thus considered to be triple-negative breast cancers (TNBC; refs. 1, 2). Although a high percentage of patients with TNBC initially respond to conventional chemotherapy, they tend to have a higher rate of relapse and worse prognosis as compared with other breast cancer subtypes (1, 2). In efforts to identify new molecular targets in TNBC, various groups have performed gene expression profiling studies and identified that the EGF receptor (EGFR) is commonly overexpressed (3–6). Although inhibition of EGFR activity has yielded modest clinical success in TNBC, substantial gains

in clinical response rates have not been achieved (7, 8). Thus, improving the efficacy of anti-EGFR therapy in TNBC is imperative.

Classically, EGFR functions as a plasma membrane-bound receptor tyrosine kinase that initiates growth and survival signals (9). However, studies over the last 15 years have identified that EGFR can be localized and function from intracellular organelles, one of which includes the nucleus (10, 11). Within the nucleus, EGFR can function as a cotranscription factor to regulate genes involved in tumor progression (10, 11), in addition to functioning as a nuclear kinase to enhance DNA replication and repair (12–14). These nuclear functions have been linked to three parameters of tumor biology: (i) inverse correlation with overall survival in numerous cancers (15–20), (ii) resistance to therapeutic agents including radiation (12, 21–24), chemotherapy (12, 13, 24), and anti-EGFR therapies gefitinib (25) and cetuximab (26), and (iii) enhanced tumor growth (27, 28). These findings suggest that tumors rely on two distinct compartments of EGFR signaling to sustain their oncogenic phenotype: (i) classical membrane-bound EGFR signaling, and (ii) nuclear EGFR (nEGFR) signaling.

Previous work from our laboratory has identified that non-small cell lung cancer (NSCLC) cells that have acquired resistance to cetuximab express increased nEGFR and Src Family Kinase (SFK) activity (26, 29). SFK inhibition blocked nEGFR translocation in cetuximab-resistant

**Authors' Affiliations:** Departments of <sup>1</sup>Human Oncology and <sup>2</sup>Pathology and Laboratory Medicine, University of Wisconsin School of Medicine and Public Health, <sup>3</sup>Department of Medicine, University of Wisconsin Carbone Cancer Center, Madison, Wisconsin; and <sup>4</sup>Division of Hematology/Oncology, Department of Medicine, University of Chicago, Chicago, Illinois

**Note:** Supplementary data for this article are available at Molecular Cancer Therapeutics Online (<http://mct.aacrjournals.org/>).

**Corresponding Author:** Deric L. Wheeler, University of Wisconsin, 1111 Highland Ave, WIMR 3159, Madison, WI 53705. Phone: 608-262-7837; Fax: 608-263-9947; E-mail: [dlwheeler@wisc.edu](mailto:dlwheeler@wisc.edu)

doi: 10.1158/1535-7163.MCT-13-1021

©2014 American Association for Cancer Research.

cells, and led to an increase in plasma membrane EGFR expression and enhanced sensitivity to cetuximab (26, 30). Furthermore, the SFK-dependent phosphorylation site on EGFR, tyrosine 1101 (Y1101), was identified to play a critical role in initiating EGFR's nuclear transport (30). These studies suggest that nEGFR is a critical molecular determinant for cetuximab resistance and that SFKs play an important role in regulating nEGFR translocation.

On the basis of these previous studies, we hypothesized that nEGFR may promote intrinsic resistance to cetuximab in TNBC. To examine this question, a battery of TNBC cell lines and human tumors were screened and found to express nEGFR. Although TNBC cell lines were notably resistant to cetuximab therapy, all lines retained dependency on EGFR for proliferation. Furthermore, SFKs influenced nEGFR transport in TNBC, where the overexpression of a negative regulator of Src decreased EGFR activity at tyrosine 1101 and inhibited nEGFR translocation. Interestingly, the creation of stable cell lines overexpressing each SFK demonstrated that all SFKs could promote nEGFR translocation. Treatment of TNBC cell lines and xenograft tumors with the anti-SFK therapeutic dasatinib inhibited nEGFR translocation, and enhanced surface level EGFR accumulation. Importantly, pretreatment of TNBC cell lines with dasatinib greatly enhanced the sensitivity of cetuximab-resistant TNBC cell lines to cetuximab. Collectively, our data suggest that abrogating nEGFR translocation with SFK inhibitors may greatly enhance the efficacy of cetuximab in TNBC.

## Materials and Methods

### Cell lines

The human breast cancer cell lines SKBr3, BT474, BT549, MDAMB231 and MDAMB468, MCF-7, and the Chinese hamster ovary cell line CHOK1 were purchased from American Type Culture Collection in November 2010. SUM149, SUM229, and SUM159 were purchased from Asterand in November 2010. All cell lines were authenticated by the indicated source and not by our laboratory. All cell lines were maintained in their respective media (Mediatech Inc.) with 1% penicillin and streptomycin; SKBr3, BT549, and MDAMB231, Dulbecco's Modified Eagle's Medium with 10% FBS; BT474, RPMI-1640 with 10% FBS; SUM149, SUM229, and SUM159, F12K medium with 5% FBS, 1 µg/mL hydrocortisone and 5 µg/mL insulin; MDAMB468 and MCF-7, DMEM/F12K medium with 10% FBS; CHOK1 F12K medium with 10% FBS.

### Antibodies, compounds, and TMAs

All antibodies were obtained from the following sources: EGFR (SC-03), pEGFR-1173 (SC-10168), HER2 (SC-284), SLAP (SC-1215), Histone H3 (SC-8654), horseradish peroxidase-conjugated goat-anti-rabbit immunoglobulin G (IgG), goat-anti-mouse IgG, donkey-anti-goat IgG, EGFR blocking peptide (SC-03 P) purchased from Santa Cruz Biotechnology Inc. SFK (CS2123), pSFK-Y419 (CS2101), pEGFR-Y1045 (CS2237), pEGFR-Y1068 (CS3777),

pHER2-Y1221/1222 (CS2243), c-Cbl (CS2747), glyceraldehyde-3-phosphate dehydrogenase (GAPDH; CS2118), calnexin (CS2679), and anti-Flag (CS8146) purchased from Cell Signaling Technology. pEGFR-Y1101 (ab76195) and EGFR (ab52894) purchased from Abcam. α-Tubulin purchased from Calbiochem. Dasatinib (BMS-354825, Sprycel) was purchased from LC Laboratories and cetuximab (C225, Erbitux) was purchased from University of Wisconsin Pharmacy (Madison, WI). EGF was purchased from Millipore. Two human TNBC tissue microarrays (TMA; #69571112B and #69572306) were purchased from TriStar Technology Group.

### Cellular fractionation and immunoblotting analysis

Cellular fractionation and whole-cell lysis were performed and quantitated as previously described (26, 31). ECL chemiluminescence detection system was used to visualize proteins. α-Tubulin, calnexin, and Histone H3 were used as loading and purity controls, respectively.

### Immunoprecipitation

Cells were processed for immunoprecipitation as previously described (31). Of note, 250 µg of protein and 2 µg of Src-like adaptor protein (SLAP) primary antibody were used for immunoprecipitation.

### Plasmids constructs, transfection, and siRNA technology

The following vectors were kindly supplied: pcDNA3.0-caSrc, -wtSRC and -EGFR wild-type (WT) and -EGFR-Y1101F, Dr. J. Boerner (Wayne State University School of Medicine, Karmanos Cancer Institute, Detroit, MI); pcDNA3-SLAP, Dr. S. Roche (Centre de Recherche de Biochimie Macromoléculaire, Montpellier, France); pTRE2pur-HA-Fyn, -Hck, and -Lck, Dr. P.S. Mischel (University of California, San Diego, La Jolla, CA). WT human pDONR223-FGR (Plasmid 23877) and pDONR223-Blk (Plasmid 23940) were purchased from Addgene. pQCXIP-YES and -LYN as previously described (30). All SFKs were subcloned into the PAC1/AGEI restriction sites of the pQCXIP expression vector (Clontech). Both transient and stable transfections were performed using Lipofectamine LTX and Opti-MEM I (Life Technology). Stable transfection was commenced 48 hours posttransfection via addition of 500 ng/mL puromycin to the growth media. Single cell clones were chosen for expansion and validation for specific SFK expression.

For siRNAs, cells were transfected with 30 nmol/L siEGFR (ON-TARGETplus, SMART pool #L-003114-00, Dharmacon) or siNon-targeting (NT; ON-TARGETplus Non-targeting Pool, D-001810, Dharmacon) using Lipofectamine RNAiMAX (Life Technology) according to the manufacturer's instructions. Vehicle (Veh)-treated cells were treated with RNAiMAX only.

### Cell proliferation assay

Crystal violet assay and Cell Counting Kit-8 (Dojindo Molecular Technologies) were performed as previously



described (26, 32). Cellular proliferation was measured 72 to 96 hours post siRNA and 96 hours post drug treatment.

### Transmission electron microscopy

Cells were plated on glass cover slips at approximately 90% confluency. The pre-embedding labeling method was used for processing as previously described (33). Specifically, 0.8% Triton X-100 was used for permeabilization and 7 µg/mL of EGFR primary antibody was used (SC-03, Santa Cruz Biotechnology). Cells were silver enhanced for 1.5 hour. Cells were sectioned onto copper grids at approximately 90 nm slices.

### Immunofluorescence

Cells were processed for immunofluorescence staining of EGFR as previously described (31). Primary antibody: EGFR (SC-03), 1:100. Secondary antibody (Life technologies): Alex Fluor 546 at 1:600 for 30 minutes to 1 hour. All cells were mounted with ProLong Gold Antifade Reagent with 4', 6-diamidino-2-phenylindole (DAPI; Life Technologies). Confocal immunofluorescence microscopy was performed using an A1 Nikon confocal microscope (×600). Z-slices were taken at 150 nm slices.

### Nuance imaging analysis

For image analysis, EGFR (ab52894, 1:50) and anti-E Cadherin antibody (NCH-38, Dako at 1:100 dilution) were used for immunofluorescence staining. Images were acquired on the Nuance Multispectral Imaging System (Caliper Life Sciences, ×200). A spectral library composed of the fluorescent spectrum of each fluorophore was constructed from vehicle treated cells stained with each fluorophore individually. Images were analyzed on the inForm Image Analysis Software (Caliper Life Sciences) as previously described (34) by pathologist D. Yang. Relative expression of EGFR in each compartment was expressed as a ratio of proportion of counts in the high intensity bins (bins 6–10) divided by the proportion of counts in the low intensity bins (bins 1–5).

### Immunohistochemistry

Cells were processed for immunohistochemistry (IHC) as previously described (32). EGFR antibody (SC-03) was used at a 1:100 dilution. The nEGFR staining pattern was scored by pathologist (D. Yang) analysis at 5% increments by visual estimation at ×20 magnification. Cases with at least one replicate core containing at least 5% of tumor cells demonstrating strong nEGFR IHC protein expression were scored as nEGFR positive.

### Flow cytometry

Cells were processed as previously described (26). Cells were analyzed using a FACSCalibur flow cytometer (BD Biosciences). Propidium iodide was added to each sample at a final concentration of 5 mg/mL. Histogram analysis was performed using FlowJo software (Tree Star Inc.).

### Mouse xenograft model and tumor collection

Athymic nude mice (4–6-week-old females) were obtained from Harlan Laboratories. All animal procedures and maintenance were conducted in accordance with the institutional guidelines of the University of Wisconsin. Twelve mice were injected in the dorsal flank with  $2 \times 10^6$  MDAMB468 cells. Once tumors reached 100 mm<sup>3</sup>, mice were randomized into treatment groups: vehicle (sodium citrate monobasic buffer) or dasatinib (50 mg/kg/d). Mice were treated once daily for 4 days via oral gavage. Tumor volume measurements were evaluated by digital calipers and calculated by the formula  $(\pi/6 \times (\text{large diameter}) \times (\text{small diameter})^2)$ . Tumors were collected, processed, and stained as previously described (32, 35).

### Statistical analysis

Student *t* tests were used to evaluate the significance in proliferation rate between vehicle and siEGFR or drug-treated cells. Student *t* tests were also used to evaluate significance in nEGFR expression levels by Nuance imaging analysis between vehicle- and dasatinib-treated cells. Differences were considered statistically significant if \*, *P* < 0.05. Pearson correlation coefficient and Manders' overlap coefficient for colocalization were calculated using Nikon NIS-Elements software. Significance of strong interaction is considered for values ≥0.5 (36).

## Results

### TNBC cell lines and human tumors express nuclear localized EGFR

Six established TNBC cell lines were evaluated for EGFR expression (Fig. 1A). All cell lines expressed total and activated forms of EGFR, in which the autophosphorylation status of EGFR at tyrosine 1068, 1173, and 1045, as well as the SFK-specific phosphorylation site, tyrosine 1101, were evaluated. All TNBC cell lines expressed activated SFKs, as observed in previous studies (refs. 37, 38; Fig. 1A). Total and activated HER2 expression levels were low in all TNBC cell lines compared with HER2-positive cell lines SKBr3 and BT474.

Because TNBC cell lines expressed EGFR, we hypothesized that some cell lines may also express nEGFR. Variant levels of nEGFR expression were observed in TNBC cell lines by nuclear fractionation analysis (Fig. 1B). The harvested nuclear lysate was free from contaminating cytoplasmic and ER-associated proteins, as indicated by lack of α-tubulin and calnexin. The nuclear protein Histone H3 was used as a loading and nuclear protein purity control. In addition, confocal immunofluorescent microscopy indicated strong nEGFR immunofluorescent staining in MDAMB468, SUM229, and SUM149 cells (Fig. 1B) by merging DAPI and Alexa Fluor 546-labeled EGFR (white arrows, magnified image). Statistical significance of colocalization was analyzed by Pearson and Manders' correlation coefficients (significance of a strong interaction is



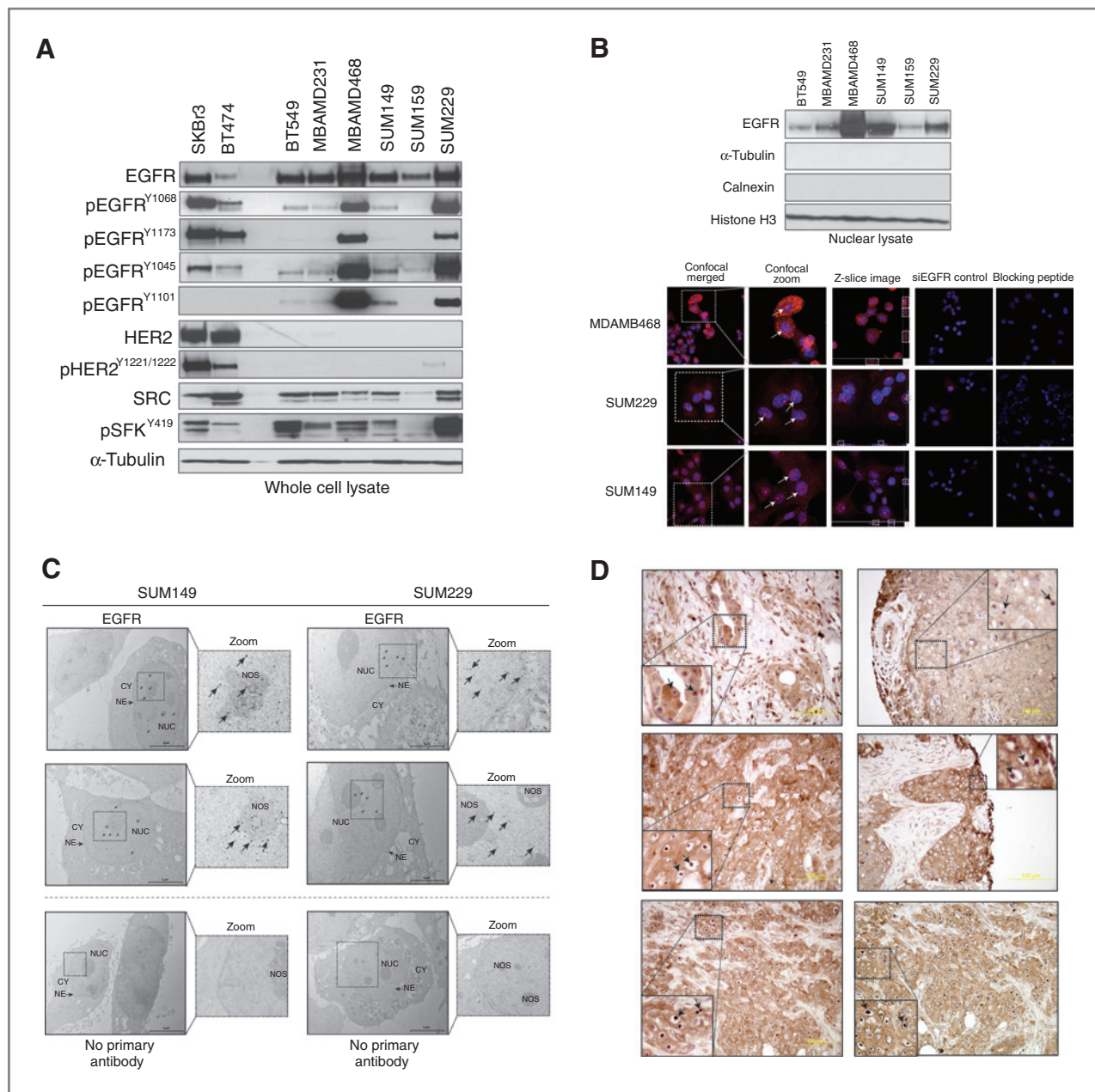


**Figure 1.** TNBC cell lines and human tumors express nuclear localized EGFR. **A**, TNBC cells express total and activated forms of EGFR. Whole-cell lysate was harvested from six TNBC cell lines and two HER2-positive cell lines.  $\alpha$ -Tubulin was used as a loading control. **B**, TNBC cells express nEGFR. Cell lines were harvested for nuclear proteins.  $\alpha$ -Tubulin, calnexin, and Histone H3 were used as loading and purity controls, respectively. Confocal immunofluorescence (IF) microscopy depicts nEGFR expression. Merged images were magnified to depict nEGFR (confocal zoom, white arrows). A single Z-Slice image depicts overlap between blue and red signal (white dashed-line boxes).  $\times 600$  magnification. EGFR primary antibody specificity was validated with siEGFR and blocking peptides. **C**, immunogold labeling of nEGFR. TNBC cells were fixed and processed for transmission EM. CY, cytoplasm; NE, nuclear envelope; NUC, nucleus; NOS, nucleolus. Images were digitally zoomed to highlight gold particles in the nucleus (black arrows). **D**, human TNBC tumors express nEGFR. Immunohistochemical staining for EGFR was performed on a total of 74 TNBC patient tumor sections. Representative cases demonstrating nEGFR expression are depicted (black arrows).

$\geq 0.5$ ; ref. 36). For MDAMB468, SUM229, and SUM149, the Pearson coefficients were  $0.52 \pm 0.04$ ,  $0.58 \pm 0.01$ , and  $0.65 \pm 0.02$ , and the Manders' overlap coefficients were  $0.70 \pm 0.02$ ,  $0.78 \pm 0.03$ , and  $0.84 \pm 0.01$  ( $n = 50$  cells). Although homogenous nEGFR staining was observed in SUM149

and SUM229 cells by immunofluorescence, nEGFR staining in MDAMB468 cells was more heterogeneous. Knock-down of EGFR using siRNA or preincubation of primary antibody with blocking peptides led to dramatic decreases in EGFR signal. There was no signal detected from cells

incubated with secondary antibody only (data not shown). We further validated nEGFR expression using transmission electron microscopy (Fig. 1C). EGFR labeled with immunogold conjugated secondary antibodies indicated that EGFR was indeed localized in the nucleus, with localization in the nucleolus and around the nuclear envelope.

Given that nEGFR was expressed in established TNBC cell lines, we probed a human TMA containing 74 TNBC patient tumors for EGFR expression and localization. Pathologist analysis of tumors stained for EGFR via IHC indicated that 19% of the tumors expressed nEGFR (Fig. 1D). Interestingly, nEGFR was highly localized to the nucleolus in more than 5% of nEGFR-positive tumors. In addition, some tumor sections contained concentrated nEGFR, whereas other areas of the same tumor lacked nEGFR expression. There was no signal detected from cores stained with secondary antibody only (data not shown). Collectively, these data demonstrate that TNBC cell lines and human tumors express nEGFR.

#### **TNBC cells are resistant to cetuximab therapy, but dependent on EGFR for proliferation**

To determine the role of EGFR in TNBC proliferation, studies were performed to knock down EGFR expression in various TNBC cell lines using an EGFR-directed siRNA pool. Loss of EGFR expression led to a 23% to 50% reduction in cell proliferation as compared to cells treated with vehicle or NT siRNA (Fig. 2). Each cell line challenged with increasing doses of cetuximab (from 0.01 nmol/L to 100 nmol/L) demonstrated only minor reductions in proliferation. The cell lines MDAMB231 (Fig. 2B) and MDAMB468 (Fig. 2D) demonstrated a 15% reduction in proliferation upon treatment with 100 nmol/L of cetuximab, whereas the SUM159 (Fig. 2A), SUM229 (Fig. 2C), and SUM149 (Fig. 2E) were unaffected at this dose. In addition, TNBC cell lines treated with increasing doses of dasatinib (0.01–100 nmol/L) were relatively resistant to growth inhibition. These results indicate that TNBC cell lines depend on EGFR for proliferation but are relatively resistant to cetuximab.

#### **SFKs mediate the nuclear translocation of EGFR in TNBC**

Previous studies from our laboratory indicate that SFKs influence nEGFR translocation in lung cancer (26, 30). To investigate whether SFKs influence EGFR translocation from the plasma membrane to the nucleus in TNBC, constitutively active Src (caSrc) was overexpressed in SUM159, BT549, and MDAMB231 cells. The overexpression of caSrc, indicated by enhanced pSFK-Y419, led to increases in nEGFR expression (Fig. 3A). Next, a negative regulator of Src, SLAP (39), was overexpressed in SUM149, SUM229, and MDAMB468 cells. The overexpression of SLAP, indicated by the expression of the Flag tag, led to decreases in nEGFR levels (Fig. 3B). These studies indicate that modulation of SFK activity can influence nEGFR expression in TNBC cell lines.

Previous studies elucidating the functions of SLAP have identified that SLAP functions as an antagonist for Src-induced mitogenesis partly through the binding of Src substrates and effector molecules (39). Overexpression of SLAP resulted in its association with EGFR in three TNBC cell lines by coimmunoprecipitation analysis (Fig. 3C). Immunoprecipitation with an IgG control yielded no signal (data not shown). Because EGFR deficient in tyrosine 1101 (Y1101) phosphorylation is hindered in nuclear translocation (Fig. 3C, Inset 1; ref. 30), we probed for phosphorylated EGFR at Y1101 post SLAP transfection. Indeed, TNBC cell lines overexpressing SLAP had decreased phosphorylation of EGFR at Y1101 (Fig. 3C), which correlated with decreased nEGFR (Fig. 3B). These data demonstrate that SFK phosphorylation of EGFR at Y1101 can influence nEGFR translocation in TNBC.

#### **SFKs exhibit functional redundancy in their ability to influence nEGFR translocation**

Previous reports suggest that the SFKs Yes and Lyn play a role in the nuclear translocation of EGFR (30). However, experiments in Fig. 3 indicated that caSrc and SLAP could influence nEGFR translocation in TNBC cells, suggesting that global increased activity of SFKs may influence nEGFR expression. To test this hypothesis, stable clones of individual SFKs (Src, Yes, Lyn, Lck, Hck, Fyn, Blk, and Fgr) were engineered in the breast cancer cell line MCF-7. One or two stable clones were chosen for each SFK for comparison with an empty vector stable cell line (Fig. 4A). The overexpression of each SFK led to the enhanced expression and nuclear translocation of EGFR. All cell lines were stimulated with 5 nmol/L EGF to promote the nuclear translocation of EGFR; however, a basal level of nEGFR was detected in nonstimulated SFK stable cells (data not shown). In addition, the stable overexpression of each SFK led to their increased activation, corresponding to a downregulation of the E3 ubiquitin ligase, c-Cbl (Fig. 4B). This result may explain why an increase in total EGFR was observed in Fig. 4A. Collectively, these data suggest that SFKs play functional redundant roles in promoting nEGFR translocation.

#### **Therapeutic inhibition of SFKs can block nEGFR translocation in *in vitro* and *in vivo* TNBC tumor models**

Because the modulation of SFK activity influenced nEGFR, the SFK inhibitor dasatinib was utilized to determine whether it could abrogate EGFR translocation from the membrane to nucleus. Treatment of TNBC cells with dasatinib led to potent decreases in nEGFR levels (at 24 and 72 hours in SUM149 and SUM229, and at 72 hours in MDAMB468 cells; Fig. 5A). Analysis of whole-cell lysate indicated that EGFR activity on Y1101 was inhibited by dasatinib at both time points. In addition, dasatinib treatment led to subsequent increases in non-nEGFR levels (Fig. 5A). Nuance imaging and Inform software was further used to analyze nEGFR levels post-dasatinib treatment (Fig. 5B). Cells were stained for EGFR, E-Cadherin, and DAPI; E-Cadherin and DAPI were used to create a spectral

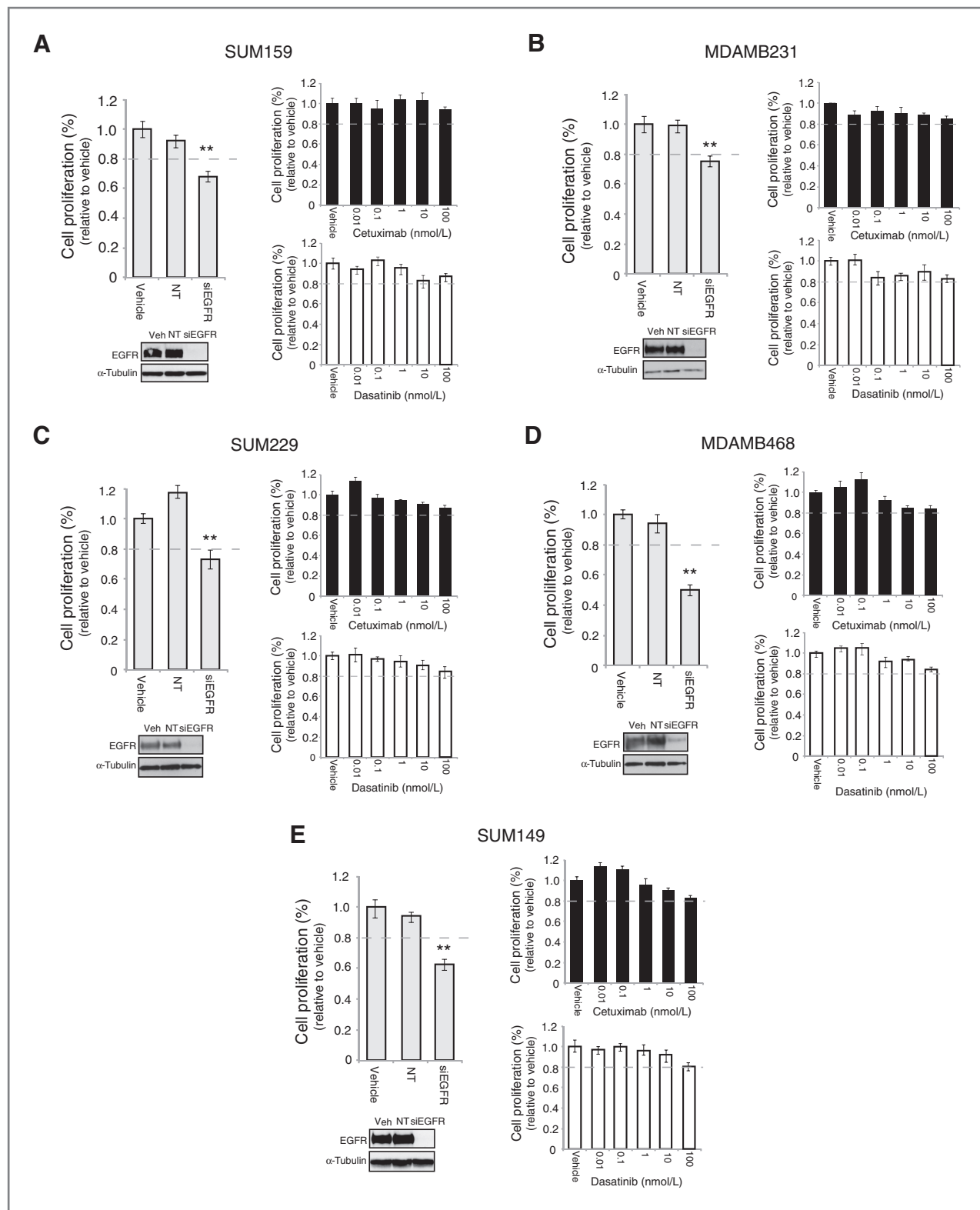


**Figure 2.** TNBC cell lines are dependent on EGFR for proliferation, but are intrinsically resistant to cetuximab and dasatinib. Cell lines were incubated with siEGFR, nontargeting (NT) siRNA, or vehicle for 72 to 96 hours before performing proliferation assays (A–E). Cells were treated with cetuximab or dasatinib at indicated doses for the same time course. Proliferation is plotted as a percentage of growth relative to vehicle-treated cells ( $n = 3$ ). Whole-cell lysate was harvested from all cell lines at the same time point to confirm knockdown of EGFR. Data, mean  $\pm$  SEM. \*\*,  $P < 0.01$ .

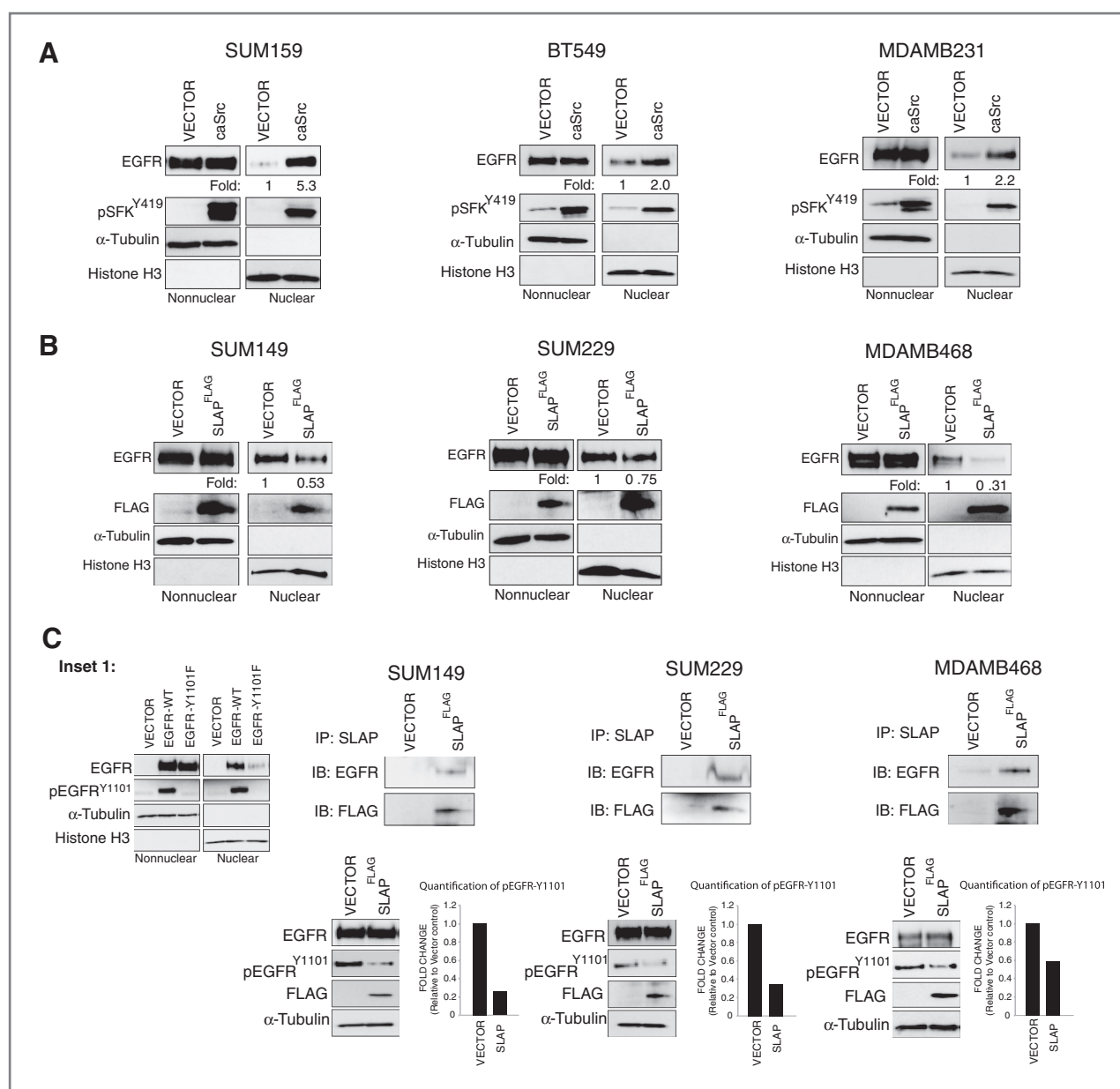


**Figure 3.** SFKs mediate nEGFR translocation in TNBC. **A**, constitutively active Src (caSrc) enhances nEGFR translocation in TNBC cell lines. Cells were transfected with caSrc or an empty vector control for 48 hours before stimulation with EGF (5 nmol/L, 45 minutes) to induce nEGFR translocation. Nonnuclear and nuclear proteins were harvested. nEGFR expression was quantitated using ImageJ software. **B**, a negative regulator of Src, SLAP, blocks nEGFR translocation in TNBC cell lines. Cells were transfected with SLAP-FLAG or an empty vector control for 48 hours before harvesting nonnuclear and nuclear proteins. nEGFR expression was analyzed. **C**, SLAP can interact with EGFR and decrease EGFR activation at tyrosine 1101. Cells were transfected with SLAP-FLAG or an empty vector control for 48 hours before harvesting whole-cell lysate. 250  $\mu$ g of cell lysate was immunoprecipitated with an anti-SLAP antibody. The same lysate was subjected to immunoblot analysis for activation of EGFR at tyrosine 1101. pEGFR-Y1101 activity was quantitated using ImageJ software. Inset 1, EGFR mutated at tyrosine 1101 is deficient in nuclear localization. Vector, EGFR-WT, and EGFR-Y1101F were transfected into CHOK1 cells for 48 hours before stimulation with EGF (5 nmol/L, 45 minutes). Nonnuclear and nuclear proteins were harvested, and nEGFR expression was analyzed.

library that segmented each cell into cytoplasm and nucleus as previously described (34). InForm software analysis of each cell line ( $n = 2$ ) demonstrated that dasatinib-treated cells trended toward less nEGFR staining as compared with vehicle-treated cells ( $P = 0.08$  at 48 hours).

To further characterize the effect of dasatinib on non-nEGFR expression, surface level EGFR was analyzed by

flow cytometry. TNBC cells treated with dasatinib for 24 hours contained 30% to 42% more plasma membrane-bound EGFR as compared with vehicle-treated cells (Fig. 5C). There was no additional increase in EGFR surface expression 72 hours posttreatment (data not shown). Together, these data suggest that EGFR accumulates on the plasma membrane when nEGFR translocation is blocked by dasatinib.



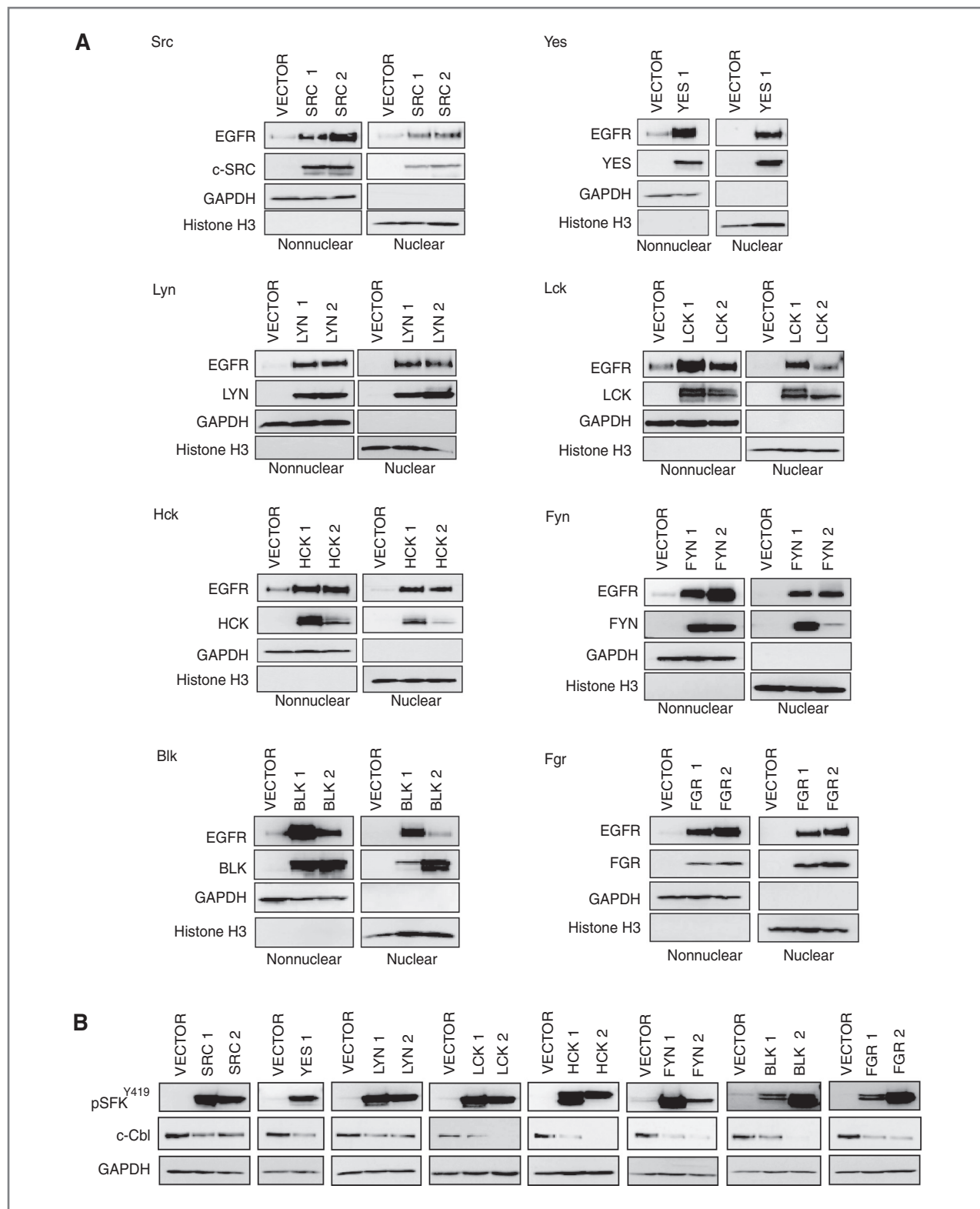


**Figure 4.** SFKs exhibit functional redundancy in their ability to influence nEGFR translocation. **A**, the stable overexpression of SFKs increase nEGFR expression. Eight different SFKs were stably overexpressed in the breast cancer cell line MCF-7. SFK stable clones or an empty vector stable cell line were stimulated with EGF (5 nmol/L, 45 minutes) to induce nEGFR translocation, before harvesting nonnuclear and nuclear proteins. GAPDH and Histone H3 were used as loading and purity controls, respectively. **B**, the stable overexpression of SFKs downregulate c-Cbl. Whole-cell lysate was harvested from SFK stable clones or an empty vector stable cell line. GAPDH was used as loading control.

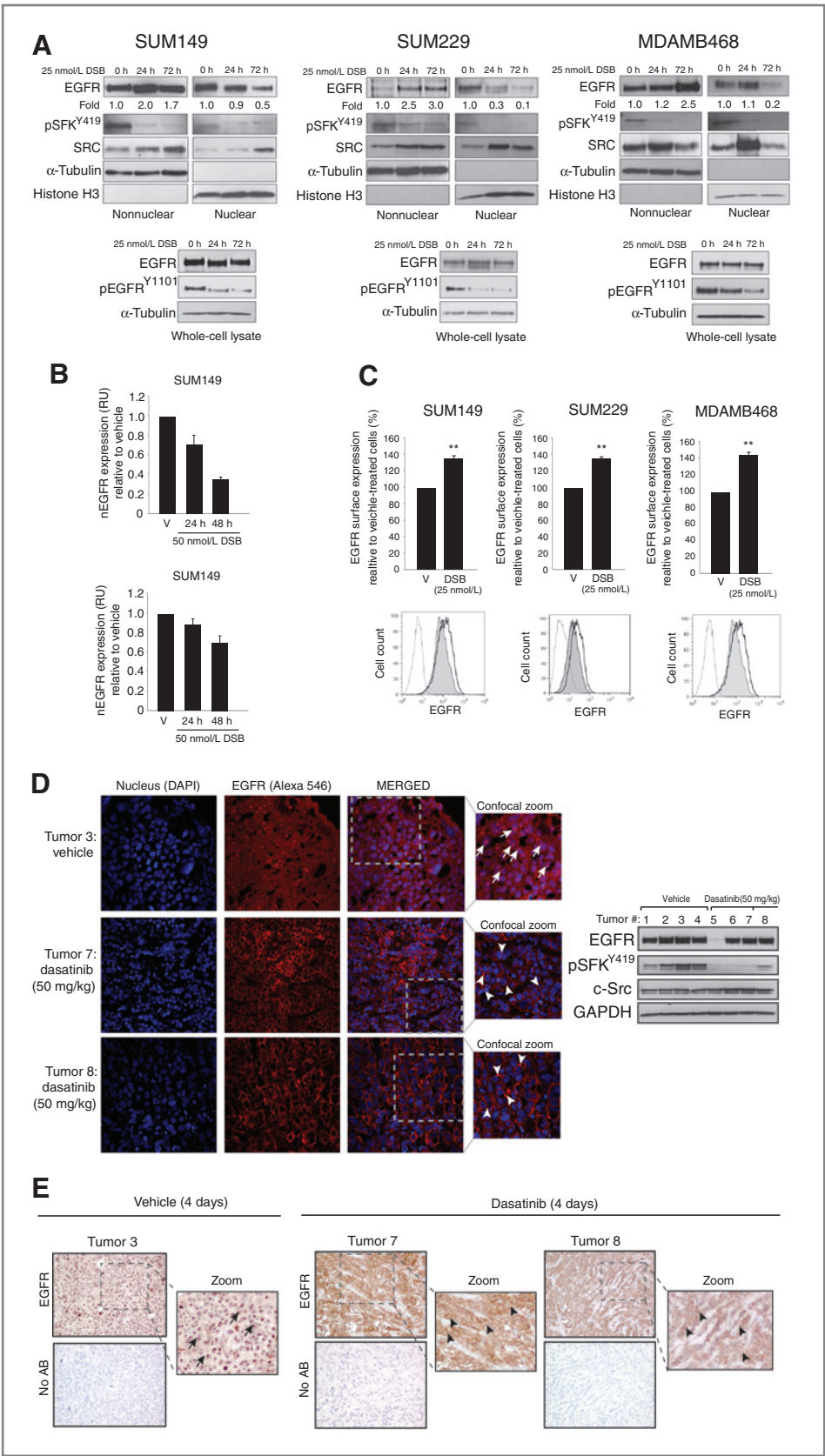


**Figure 5.** Therapeutic inhibition of SFKs can block nEGFR translocation in TNBC cell lines and tumor models. **A**, dasatinib can inhibit nEGFR translocation and enhance nonnuclear EGFR levels. Cells were treated with vehicle or dasatinib (25 nmol/L) for 24 and 72 hours before harvesting whole cell, nonnuclear, and nuclear proteins. **B**, dasatinib can block nEGFR translocation measured by Nuance imaging analysis. Cells were treated with vehicle or dasatinib (50 nmol/L) for 24 and 48 hours before staining for EGFR, E-Cadherin, and DAPI. nEGFR fluorescence detected from dasatinib-treated cells was normalized to nEGFR fluorescence detected from vehicle-treated cells using InForm software ( $n = 2$ ). **C**, dasatinib can enhance plasma membrane-bound EGFR levels measured by flow cytometry. Cells were treated with dasatinib (25 nmol/L) for 24 hours before EGFR surface level analysis. Surface level EGFR expression of dasatinib-treated cells was normalized to vehicle-treated cells ( $n = 3$ ). Shaded histogram, vehicle-treated cells; nonshaded histograms, dasatinib-treated cells. IgG-treated cells are used as a control (dotted line). **D** and **E**, dasatinib can block nEGFR translocation in MDAMB468 xenograft tumors. Mice with established MDAMB468 tumors were treated with 50 mg/kg of dasatinib or vehicle once a day for 4 days. Tumors were analyzed by confocal immunofluorescence (IF; **D**) and IHC (**E**) for EGFR expression. IF, merged images were magnified to depict nEGFR (arrows) and non-nEGFR (triangle).  $\times 600$  magnification for IF and  $\times 400$  for IHC. Four tumors from vehicle (tumor # 1–4) or dasatinib-treated mice (tumor # 5–8) were harvested for protein and analyzed for the indicated proteins. Data, mean  $\pm$  SEM. \*\*,  $P < 0.01$ .

To investigate whether therapeutic inhibition of SFKs can abrogate nEGFR translocation *in vivo*, MDAMB468 cells were established as xenograft tumors in female athymic nude mice. Mice were randomized into two groups receiving 50 mg/kg of dasatinib or vehicle once daily for 4 days. Figure 5D represents confocal immunofluorescence analyses of representative tumor sections harvested from either vehicle- or dasatinib-treated mice stained for EGFR. EGFR was highly nuclear localized in tumors from vehicle-treated mice. However, tumors harvested from dasatinib-treated mice harbored much less nEGFR, with a noticeable increase in plasma membrane localized EGFR expression. Immunoblot analysis of harvested tumors validated that dasatinib inhibited SFK activity; one dasatinib-treated tumor (#5) contained less total EGFR expression. The inhibition of nEGFR translocation was also visualized by immunohistochemical staining of tumors harvested from dasatinib-treated mice (Fig. 5E). Interestingly, we found that dasatinib treatment of

mice harboring colorectal tumors also contained less nEGFR expression within the tumor (Supplementary Fig. S1), suggesting that SFKs may influence nEGFR translocation in different tumor types. Collectively, these data indicate that SFK inhibition prevents nEGFR translocation and enhances membrane accumulation of EGFR *in vivo*.

#### SFK inhibition can sensitize TNBC cells to cetuximab growth inhibition

Because SFK inhibition enhanced plasma membrane-bound EGFR expression, we hypothesized that TNBC cells may become more sensitive to cetuximab upon pretreatment with dasatinib. To investigate this, we performed proliferation assays after pretreating TNBC cells with dasatinib or vehicle for 24 hours, the time point at which an increase in surface level EGFR was detected, and subsequently treating cells with increasing doses of cetuximab for an additional 72 hours (Fig. 6). All cell lines pretreated with vehicle and subsequently treated

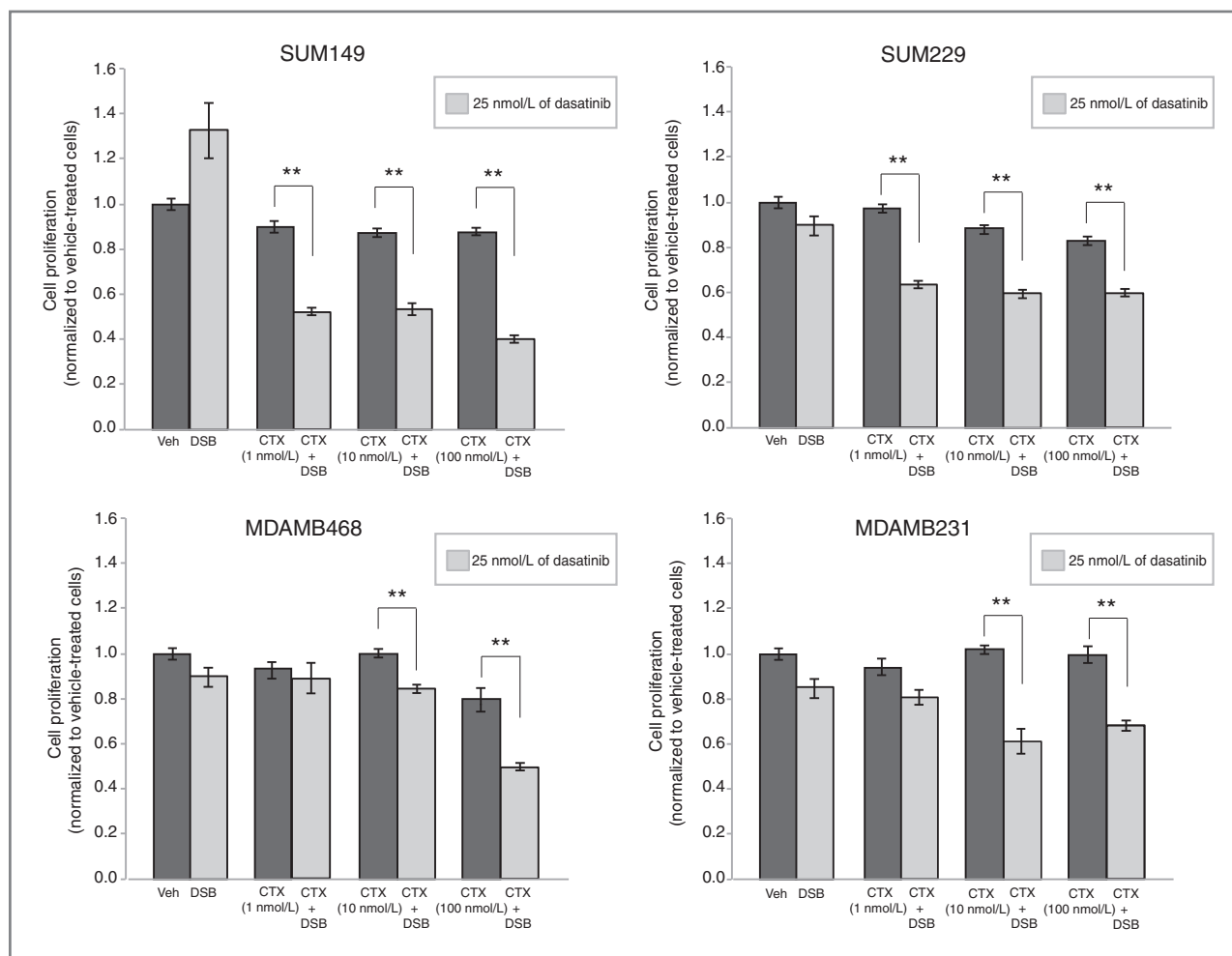


**Figure 6.** Therapeutic inhibition of SFK activity can sensitize TNBC cells to cetuximab. Cells were pretreated with vehicle or dasatinib (25 nmol/L) for 24 hours before adding cetuximab to the growth medium at the indicated doses (1, 10, and 100 nmol/L) for an additional 72 hours. Proliferation assays were performed and plotted as a percentage of growth relative to vehicle-treated cells ( $n = 3$ ). Data, mean  $\pm$  SEM. \*\*,  $P < 0.01$ .



with increasing doses of cetuximab demonstrated minor reductions in proliferation, consistent with data in Fig. 2. In addition, cells treated with 25 nmol/L dasatinib monotherapy did not exhibit significant inhibition of proliferation. However, TNBC cell lines that received dasatinib for 24 hours before cetuximab treatment demonstrated significant reductions in proliferation over a wide range of cetuximab doses (1–100 nmol/L). SUM149 and SUM229 cells demonstrated significant reductions in proliferation at low doses of cetuximab (1 nmol/L), whereas MDAMB468 and MDAMB231 cells exhibited proliferation inhibition at higher doses of cetuximab (10 and 100 nmol/L). Collectively, these data suggest that the blockade of nEGFR translocation via SFK inhibition can increase TNBC cell sensitivity to cetuximab.

## Discussion

TNBC is a subset of breast cancers that commonly overexpress the EGFR (3–6). Unfortunately, clinical trials targeting EGFR with cetuximab have yielded minimal benefit in TNBC (7, 8), even with the addition of platinum-based chemotherapies (1, 5, 36). Thus, understanding why TNBCs are intrinsically resistant to cetuximab has become an important clinical question. Over the last decade, numerous studies have identified a role for nEGFR in resistance to anti-EGFR agents (25, 26). Previous studies from our laboratory demonstrated that NSCLC cell lines that had acquired resistance to cetuximab relied on nEGFR signaling to maintain their resistant phenotype (26). On the basis of these studies, we hypothesized that nEGFR may be a critical molecular determinant for cetuximab resistance in TNBC.

In the current study, nEGFR was detected in a panel of established TNBC cell lines and human tumors (Fig. 1). In prior studies, 38% of a 130 breast cancer patient cohort (15) and 40% of a 113 breast cancer patient cohort (19) stained positive for nEGFR, which was further correlated with worse overall survival. The heterogeneity observed in nEGFR expression in the current study of TNBC tumors highlights the importance of simultaneously targeting both nEGFR and non-nEGFR cell populations. Another interesting observation lies in the localization of EGFR in the nucleolus, functions that have yet to be investigated and may be playing important roles in TNBC pathogenesis. Collectively, the preclinical data presented in the current study suggest that nEGFR may be indicative of cetuximab-resistant tumors warranting further investigation for its role as a predictive marker for cetuximab response in TNBC.

Recent work from our laboratory has found that SFK-dependent phosphorylation of EGFR on Y1101 is a necessary and early event for EGFR translocation from the plasma membrane to the nucleus (30). The current study aimed to identify whether this mechanism of nuclear translocation was present in TNBC. We found that three TNBC cell lines (MDAMB468, SUM149, and SUM229) with the highest levels of phosphorylated Y1101 also expressed the highest levels of nEGFR (Fig. 1A and B). In addition,

inhibition of SFK activity led to decreased phosphorylation of EGFR on Y1101 and reduced nEGFR levels (Figs. 3C and 5A and B). Interestingly, Fig. 5C indicates that surface level EGFR was enhanced within 24 hours of dasatinib treatment, even though a decrease in nEGFR expression was more prominent at later time points posttreatment (Fig. 5A and B); this suggests that the rate of nEGFR export, via its nuclear export sequence (28), varies between cell lines. Collectively, these data suggest that SFK phosphorylation of EGFR on Y1101 may be a critical step for EGFR nuclear translocation in TNBC.

SFKs consist of 11 intracellular tyrosine kinases that are differentially expressed in a variety of cancers (40). In the current study, eight individual SFKs were stably overexpressed, and found to function similarly in their ability to influence (i) the steady state expression of total EGFR, (ii) nEGFR translocation, and (iii) degradation of c-Cbl (Fig. 4). These data suggest that SFKs exhibit functional redundancy in their ability to influence nEGFR translocation, and thus the use of broad-spectrum SFK inhibitors, such as dasatinib, may be highly beneficial in nEGFR-positive cancers.

In the current study, SFK inhibition of nEGFR translocation led to an accumulation of plasma membrane-bound EGFR and sensitization to cetuximab therapy (Figs. 5 and 6). Recent studies support our findings, where antitumorigenic effects of both cetuximab and dasatinib dual treatment with chemotherapy (41) and the use of noncompetitive monoclonal antibodies degrading the EGFR (42) have been documented in TNBC. In addition, a recent report demonstrated that targeting PCNA, a nEGFR substrate, could delay TNBC tumor growth (43). In the current study, sensitization to cetuximab was observed after pretreatment of TNBC cells with dasatinib for 24 hours, the time point at which EGFR accumulation was detected on the plasma membrane due to the inhibition of nEGFR translocation. We speculate that the inhibition of nEGFR translocation drives TNBC cells to rely solely on classical membrane-bound EGFR signaling for sustained proliferation and survival signals; thus, TNBC cells become sensitized to cetuximab because cetuximab can abrogate classical EGFR signaling pathways. Previous studies in EGFR expressing NSCLC and HNSCC cell lines support this, where cell lines that lacked nEGFR expression were found to be more sensitive to cetuximab monotherapy (26, 30). Currently, the growth inhibitory effect of cetuximab and dasatinib therapy is being accessed *in vivo* TNBC models in our laboratory, a critical step for the movement of this proposed drug combination into clinical trials. Collectively, the data presented herein indicate that the dual targeting of both nEGFR and plasma membrane-bound EGFR is necessary for the complete inhibition of EGFR's oncogenic functions, a therapeutic strategy that can be readily translated for the treatment of nEGFR expressing TNBC patients.

## Disclosure of Potential Conflicts of Interest

No potential conflicts of interest were disclosed.

## Authors' Contributions

**Conception and design:** T.M. Brand, R. Salgia, D.L. Wheeler

**Development of methodology:** T.M. Brand, M. Iida, R. Salgia, D.L. Wheeler

**Acquisition of data (provided animals, acquired and managed patients, provided facilities, etc.):** T.M. Brand, M. Iida, E.F. Dunn, N. Luthar, K.T. Kostopoulos, K.L. Corrigan, D. Yang, K.B. Wisinski, R. Salgia, D.L. Wheeler

**Analysis and interpretation of data (e.g., statistical analysis, biostatistics, computational analysis):** T.M. Brand, M. Iida, K.T. Kostopoulos, R. Salgia, D.L. Wheeler

**Writing, review, and/or revision of the manuscript:** T.M. Brand, M. Iida, E.F. Dunn, N. Luthar, R. Salgia, D.L. Wheeler

**Administrative, technical, or material support (i.e., reporting or organizing data, constructing databases):** T.M. Brand, M. Iida, M.J. Wlekinski, D. Yang, D.L. Wheeler

## Acknowledgments

The authors thank Drs. Roche, Mischel, and Boerner for kindly sharing their expression vectors, Lance Rodenkirch and the Keck Laboratory for Biological Imaging for their expertise in confocal microscopy, and Ben

August and Amanda Thoma for their training and expertise in electron microscopy.

## Grant Support

This work was supported by Grant UL1TR000427 from the Clinical and Translational Science Award program, through the NIH National Center for Advancing Translational Sciences (to D.L. Wheeler), grant RSG-10-193-01-TBG from the American Cancer Society (to D.L. Wheeler), grant W81XWH-12-1-0467 from United States Army Medical Research and Materiel Command (to D.L. Wheeler), Mary Kay Foundation grant MSN152261 (to D.L. Wheeler), and NIH grant Q3 T32 GM08.1061-01A2 from Graduate Training in Cellular and Molecular Pathogenesis of Human Diseases (to T.M. Brand).

The costs of publication of this article were defrayed in part by the payment of page charges. This article must therefore be hereby marked *advertisement* in accordance with 18 U.S.C. Section 1734 solely to indicate this fact.

Received December 2, 2013; revised January 31, 2014; accepted February 16, 2014; published OnlineFirst March 14, 2014.

## References

- Schneider BP, Winer EP, Foulkes WD, Garber J, Perou CM, Richardson A, et al. Triple-negative breast cancer: risk factors to potential targets. *Clin Cancer Res* 2008;14:8010–8.
- Stevens KN, Vachon CM, Couch FJ. Genetic susceptibility to triple-negative breast cancer. *Cancer Res* 2013;73:2025–30.
- Corkery B, Crown J, Clynes M, O'Donovan N. Epidermal growth factor receptor as a potential therapeutic target in triple-negative breast cancer. *Ann Oncol* 2009;20:862–7.
- Sorlie T, Tibshirani R, Parker J, Hastie T, Marron JS, Nobel A, et al. Repeated observation of breast tumor subtypes in independent gene expression data sets. *Proc Natl Acad Sci U S A* 2003;100:8418–23.
- Nielsen TO, Hsu FD, Jensen K, Cheang M, Karaca G, Hu Z, et al. Immunohistochemical and clinical characterization of the basal-like subtype of invasive breast carcinoma. *Clin Cancer Res* 2004;10:5367–74.
- Lehmann BD, Bauer JA, Chen X, Sanders ME, Chakravarthy AB, Shyr Y, et al. Identification of human triple-negative breast cancer subtypes and preclinical models for selection of targeted therapies. *J Clin Invest* 2011;121:2750–67.
- Masuda H, Zhang D, Bartholomeusz C, Doihara H, Hortobagyi GN, Ueno NT. Role of epidermal growth factor receptor in breast cancer. *Breast Cancer Res Treat* 2012;136:331–45.
- Gelman K, Dent R, Mackey JR, Laing K, McLeod D, Verma S. Targeting triple-negative breast cancer: optimising therapeutic outcomes. *Ann Oncol* 2012;23:2223–34.
- Yarden Y, Pines G. The ERBB network: at last, cancer therapy meets systems biology. *Nat Rev Cancer* 2012;12:553–63.
- Brand TM, Iida M, Li C, Wheeler DL. The nuclear epidermal growth factor receptor signaling network and its role in cancer. *Discov Med* 2011;12:419–32.
- Han W, Lo HW. Landscape of EGFR signaling network in human cancers: biology and therapeutic response in relation to receptor subcellular locations. *Cancer Lett* 2012;318:124–34.
- Dittmann K, Mayer C, Fehrenbacher B, Schaller M, Raju U, Milas L, et al. Radiation-induced epidermal growth factor receptor nuclear import is linked to activation of DNA-dependent protein kinase. *J Biol Chem* 2005;280:31182–9.
- Hsu SC, Miller SA, Wang Y, Hung MC. Nuclear EGFR is required for cisplatin resistance and DNA repair. *Am J Transl Res* 2009;1:249–58.
- Wang SC, Nakajima Y, Yu YL, Xia W, Chen CT, Yang CC, et al. Tyrosine phosphorylation controls PCNA function through protein stability. *Nat Cell Biol* 2006;8:1359–68.
- Lo HW, Xia W, Wei Y, Ali-Sayed M, Huang SF, Hung MC. Novel prognostic value of nuclear epidermal growth factor receptor in breast cancer. *Cancer Res* 2005;65:338–48.
- Psyri A, Yu Z, Weinberger PM, Sasaki C, Haffty B, Camp R, et al. Quantitative determination of nuclear and cytoplasmic epidermal growth factor receptor expression in oropharyngeal squamous cell cancer by using automated quantitative analysis. *Clin Cancer Res* 2005;11:5856–62.
- Li CF, Fang FM, Wang JM, Tzeng CC, Tai HC, Wei YC, et al. EGFR nuclear import in gallbladder carcinoma: nuclear phosphorylated EGFR upregulates iNOS expression and confers independent prognostic impact. *Ann Surg Oncol* 2012;19:443–54.
- Xia WY, Wei YK, Du Y, Liu JS, Chang B, Yu YL, et al. Nuclear expression of epidermal growth factor receptor is a novel prognostic value in patients with ovarian cancer. *Mol Carcinog* 2009;48:610–7.
- Hadzisejdic I, Mustac E, Jonjic N, Petkovic M, Grahovac B. Nuclear EGFR in ductal invasive breast cancer: correlation with cyclin-D1 and prognosis. *Mod Pathol* 2010;23:392–403.
- Traynor AM, Weigel TL, Oettel KR, Yang DT, Zhang C, Kim K, et al. Nuclear EGFR protein expression predicts poor survival in early stage non-small cell lung cancer. *Lung Cancer* 2013;81:138–41.
- Dittmann K, Mayer C, Fehrenbacher B, Schaller M, Kehlbach R, Rodemann HP. Nuclear EGFR shuttling induced by ionizing radiation is regulated by phosphorylation at residue Thr654. *FEBS Lett* 2010;584:3878–84.
- Dittmann K, Mayer C, Fehrenbacher B, Schaller M, Kehlbach R, Rodemann HP. Nuclear epidermal growth factor receptor modulates cellular radio-sensitivity by regulation of chromatin access. *Radiother Oncol* 2011;99:317–22.
- Dittmann K, Mayer C, Rodemann HP. Inhibition of radiation-induced EGFR nuclear import by C225 (Cetuximab) suppresses DNA-PK activity. *Radiother Oncol* 2005;76:157–61.
- Liccardi G, Hartley JA, Hochhauser D. EGFR nuclear translocation modulates DNA repair following cisplatin and ionizing radiation treatment. *Cancer Res* 2011;71:1103–14.
- Huang WC, Chen YJ, Li LY, Wei YL, Hsu SC, Tsai SL, et al. Nuclear translocation of epidermal growth factor receptor by Akt-dependent phosphorylation enhances breast cancer-resistant protein expression in gefitinib-resistant cells. *J Biol Chem* 2011;286:20558–68.
- Li C, Iida M, Dunn EF, Ghia AJ, Wheeler DL. Nuclear EGFR contributes to acquired resistance to cetuximab. *Oncogene* 2009;28:3801–13.
- Lo HW, Cao X, Zhu H, Ali-Osman F. Cyclooxygenase-2 is a novel transcriptional target of the nuclear EGFR-STAT3 and EGFRvIII-STAT3 signaling axes. *Mol Cancer Res* 2010;8:232–45.
- Gururaj AE, Gibson L, Panchabhai S, Bai M, Manyam G, Lu Y, et al. Access to the nucleus and functional association with c-Myc is required for the full oncogenic potential of DeltaEGFR/EGFRvIII. *J Biol Chem* 2013;288:3428–38.
- Wheeler DL, Iida M, Kruser TJ, Nechrebecki MM, Dunn EF, Armstrong EA, et al. Epidermal growth factor receptor cooperates with Src family

- kinases in acquired resistance to cetuximab. *Cancer Biol Ther* 2009; 8:696–703.
30. Iida M, Brand TM, Campbell DA, Li C, Wheeler DL. Yes and Lyn play a role in nuclear translocation of the epidermal growth factor receptor. *Oncogene* 2012;32:759–67.
  31. Brand TM, Iida M, Luthar N, Wleklinski MJ, Starr MM, Wheeler DL. Mapping C-terminal transactivation domains of the nuclear HER family receptor tyrosine kinase HER3. *PLoS ONE* 2013;8: e71518.
  32. Li C, Brand TM, Iida M, Huang S, Armstrong EA, van der Kogel A, et al. Human epidermal growth factor receptor 3 (HER3) blockade with U3-1287/AMG888 enhances the efficacy of radiation therapy in lung and head and neck carcinoma. *Discov Med* 2013; 16:79–92.
  33. Yi H, Leunissen JLM, Shi GM, Gutekunst CA, Hersch SM. A novel procedure for pre-embedding double immunogold-silver labeling at the ultrastructural level. *J Histochem Cytochem* 2001; 49:279–83.
  34. Huang W, Hennrick K, Drew S. A colorful future of quantitative pathology: validation of Vectra technology using chromogenic multiplexed immunohistochemistry and prostate tissue microarrays. *Hum Pathol* 2013;44:29–38.
  35. Iida M, Brand TM, Starr MM, Li C, Huppert EJ, Luthar N, et al. Sym004, a novel EGFR antibody mixture, can overcome acquired resistance to cetuximab. *Neoplasia* 2013;15:1196–206.
  36. Dunn KW, Kamocka MM, McDonald JH. A practical guide to evaluating colocalization in biological microscopy. *Am J Physiol Cell Physiol* 2011;300:C723–42.
  37. Tryfonopoulos D, Walsh S, Collins DM, Flanagan L, Quinn C, Corkery B, et al. Src: a potential target for the treatment of triple-negative breast cancer. *Ann Oncol* 2011;22:2234–40.
  38. Elsberger B, Tan BA, Mitchell TJ, Brown SB, Mallon EA, Tovey SM, et al. Is expression or activation of Src kinase associated with cancer-specific survival in ER-, PR- and HER2-negative breast cancer patients? *Am J Pathol* 2009;175:1389–97.
  39. Manes G, Bello P, Roche S. Slap negatively regulates Src mitogenic function but does not revert Src-induced cell morphology changes. *Mol Cell Biol* 2000;20:3396–406.
  40. Sen B, Johnson FM. Regulation of SRC family kinases in human cancers. *J Signal transduct* 2011;2011:865819.
  41. Kim EM, Mueller K, Gartner E, Boerner J. Dasatinib is synergistic with cetuximab and cisplatin in triple-negative breast cancer cells. *J Surg Res* 2013;185:231–9.
  42. Ferraro DA, Gaborit N, Maron R, Cohen-Dvashi H, Porat Z, Pareja F, et al. Inhibition of triple-negative breast cancer models by combinations of antibodies to EGFR. *Proc Natl Acad Sci U S A* 2013;110:1815–20.
  43. Yu YL, Chou RH, Liang JH, Chang WJ, Su KJ, Tseng YJ, et al. Targeting the EGFR/PCNA signaling suppresses tumor growth of triple-negative breast cancer cells with cell-penetrating PCNA peptides. *PLoS ONE* 2013;8:e61362.



# Cancer Research

## AXL Mediates Resistance to Cetuximab Therapy

Toni M. Brand, Mari Iida, Andrew P. Stein, et al.

*Cancer Res* Published OnlineFirst August 18, 2014.

<b>Updated version</b>	Access the most recent version of this article at: doi: <a href="https://doi.org/10.1158/0008-5472.CAN-14-0294">10.1158/0008-5472.CAN-14-0294</a>
<b>Supplementary Material</b>	Access the most recent supplemental material at: <a href="http://cancerres.aacrjournals.org/content/suppl/2014/07/23/0008-5472.CAN-14-0294.DC1.html">http://cancerres.aacrjournals.org/content/suppl/2014/07/23/0008-5472.CAN-14-0294.DC1.html</a>

<b>E-mail alerts</b>	<a href="#">Sign up to receive free email-alerts</a> related to this article or journal.
<b>Reprints and Subscriptions</b>	To order reprints of this article or to subscribe to the journal, contact the AACR Publications Department at <a href="mailto:pubs@aacr.org">pubs@aacr.org</a> .
<b>Permissions</b>	To request permission to re-use all or part of this article, contact the AACR Publications Department at <a href="mailto:permissions@aacr.org">permissions@aacr.org</a> .

# AXL Mediates Resistance to Cetuximab Therapy

Toni M. Brand<sup>1</sup>, Mari Iida<sup>1</sup>, Andrew P. Stein<sup>1</sup>, Kelsey L. Corrigan<sup>1</sup>, Cara M. Braverman<sup>1</sup>, Neha Luthar<sup>1</sup>, Mahmoud Toulany<sup>2</sup>, Parkash S. Gill<sup>3</sup>, Ravi Salgia<sup>4</sup>, Randall J. Kimple<sup>1</sup>, and Deric L. Wheeler<sup>1</sup>

## Abstract

The EGFR antibody cetuximab is used to treat numerous cancers, but intrinsic and acquired resistance to this agent is a common clinical outcome. In this study, we show that overexpression of the oncogenic receptor tyrosine kinase AXL is sufficient to mediate acquired resistance to cetuximab in models of non-small cell lung cancer (NSCLC) and head and neck squamous cell carcinoma (HNSCC), where AXL was overexpressed, activated, and tightly associated with EGFR expression in cells resistant to cetuximab (Ctx<sup>R</sup> cells). Using RNAi methods and novel AXL-targeting agents, we found that AXL activation stimulated cell proliferation, EGFR activation, and MAPK signaling in Ctx<sup>R</sup> cells. Notably, EGFR directly regulated the expression of AXL mRNA through MAPK signaling and the transcription factor c-Jun in Ctx<sup>R</sup> cells, creating a positive feedback loop that maintained EGFR activation by AXL. Cetuximab-sensitive parental cells were rendered resistant to cetuximab by stable overexpression of AXL or stimulation with EGFR ligands, the latter of which increased AXL activity and association with the EGFR. In tumor xenograft models, the development of resistance following prolonged treatment with cetuximab was associated with AXL hyperactivation and EGFR association. Furthermore, in an examination of patient-derived xenografts established from surgically resected HNSCCs, AXL was overexpressed and activated in tumors that displayed intrinsic resistance to cetuximab. Collectively, our results identify AXL as a key mediator of cetuximab resistance, providing a rationale for clinical evaluation of AXL-targeting drugs to treat cetuximab-resistant cancers. *Cancer Res*; 1–13. ©2014 AACR.

## Introduction

The TAM family of receptor tyrosine kinases (RTK) is composed of three family members: Tyro-3 (Sky), AXL (Ark or Ufo), and MerTK. Cognate ligand binding to TAM receptors on the cell surface leads to receptor dimerization, kinase domain activation, and auto/trans-phosphorylation of tyrosine residues located on each receptor's cytoplasmic tail (1). The activation of TAM receptors stimulate PI3K/AKT and Ras/Raf/Mek/Erk (MAPK) signaling cascades, leading to increased cell survival, proliferation, migration, invasion, and angiogenesis (1–4).

TAM family overexpression and activation have been observed in many human cancers (1–11). Recently, the AXL receptor has been implicated in cancer cell resistance to

anti-EGFR tyrosine kinase inhibitors (TKI; refs. 12–17) and other chemotherapeutics (10, 15, 18). Collectively, these data indicate that AXL functions as a potent oncogene that can modulate resistance to conventional and targeted cancer therapies.

Cetuximab is an anti-EGFR monoclonal antibody that has shown efficacy in treating head and neck squamous cell carcinoma (HNSCC), metastatic colorectal cancer (mCRC), and non-small cell lung cancer (NSCLC; refs. 19–26). Unfortunately, clinical studies indicate that most patients who initially respond to cetuximab eventually acquire resistance (27–29). To understand the mechanisms of acquired resistance, we previously created a model in which the cetuximab-sensitive (Ctx<sup>S</sup>) NSCLC cell line NCI-H226 was treated with increasing doses of cetuximab for a period of six months until resistant single cell clones emerged (30). Analysis of cetuximab-resistant (Ctx<sup>R</sup>) clones demonstrated that the expression of EGFR and its activation was dramatically increased because of dysregulated EGFR internalization and degradation without mutation of the receptor (30). Overall, Ctx<sup>R</sup> cells remained highly addicted to the EGFR signaling network (30–32).

On the basis of these previous findings, we investigated whether the AXL receptor played a role in cetuximab resistance. Examination of *in vitro* NSCLC and HNSCC models of acquired resistance indicated that AXL was highly overexpressed and activated in Ctx<sup>R</sup> cells. Further analysis indicated that Ctx<sup>R</sup> cells had increased dependency on AXL for cellular proliferation, EGFR activation, and MAPK signaling. AXL activity

<sup>1</sup>Department of Human Oncology, University of Wisconsin School of Medicine and Public Health, Madison, Wisconsin. <sup>2</sup>Division of Radiobiology and Molecular Environmental Research, Department of Radiation Oncology, Eberhard Karls University Tübingen, Tübingen, Germany. <sup>3</sup>Departments of Medicine and Pathology, University of Southern California, Los Angeles, California. <sup>4</sup>Department of Medicine, Division of Hematology/Oncology, University of Chicago, Chicago, Illinois.

**Note:** Supplementary data for this article are available at Cancer Research Online (<http://cancerres.aacrjournals.org/>).

**Corresponding Author:** Deric L. Wheeler, Department of Human Oncology, University of Wisconsin Comprehensive Cancer Center, 1111 Highland Avenue, WIMR 3159, Madison, WI 53705. Phone: 608-262-7837; Fax: 608-263-9947; E-mail: [dlwheeler@wisc.edu](mailto:dlwheeler@wisc.edu)

doi: 10.1158/0008-5472.CAN-14-0294

©2014 American Association for Cancer Research.



was also examined in tumors harvested from *de novo*-acquired Ctx<sup>R</sup> NCI-H226 xenografts, where AXL was highly activated and associated with the EGFR. Finally, AXL was overexpressed and hyperactivated in HNSCC patient-derived xenografts (PDX) that were intrinsically resistant to cetuximab therapy. Collectively, this work indicates that AXL plays a role in cetuximab resistance and provides rationale for the clinical evaluation of anti-AXL therapeutics for the treatment of cetuximab resistant cancers.

## Materials and Methods

### Cell lines and development of acquired resistance

The human NSCLC cell line NCI-H226 was purchased from ATCC and maintained in 10% FBS in RPMI-1640 (Mediatech Inc.) with 1% penicillin and streptomycin. The HNSCC cell line UM-SCC1 was provided by Dr. Thomas E. Carey (University of Michigan, Ann Harbor, MI) and maintained in 10% FBS in Dulbecco's Modified Eagle Medium (DMEM) with 1% penicillin and streptomycin. The development of Ctx<sup>R</sup> cells has been previously described (30–32). All Ctx<sup>R</sup> cell lines were validated to express wild-type (WT) EGFR by sequencing.

### Materials

R428 was purchased from Selleckchem and MAb173 was produced in the laboratory of Dr. Parkash Gill (Department of Medicine and Pathology, University of Southern California, Los Angeles, CA). Cetuximab (ICM-225; Erbitux) was purchased from University of Wisconsin Pharmacy. EGF was purchased from Millipore and TGF $\alpha$  was purchased from Sigma-Aldrich.

### Antibodies

All antibodies were purchased from commercial sources as indicated below:

R&D Systems: AXL (for immunoblotting) and pAXL-Y779. Cell Signaling Technology: pAXL-Y702, pEGFR-Y1068, pMAPK (T202/Y204), MAPK, p-cRAF (S289/296/301), cRAF, p-AKT (S473), AKT, p-rpS6 (S240/244), rpS6, p-c-Jun (S73), c-Jun, and GAPDH. Santa Cruz Biotechnology Inc.: pEGFR-Y1173, AXL (for immunoprecipitation), and horseradish peroxidase (HRP)-conjugated goat-anti-rabbit IgG, goat-anti-mouse IgG, and donkey-anti-goat IgG. Life Technologies: AXL (for immunofluorescence). Abcam: EGFR. Calbiochem:  $\alpha$ -tubulin.

### siRNA and transfection

Ctx<sup>R</sup> cells were transiently transfected with AXL siRNA (siAXL; ON-TARGETplus, SMARTpool #L-003104; Dharmacon), siEGFR (ON-TARGETplus, SMARTpool #L-003114; Dharmacon), siHER2 (ON-TARGETplus, SMARTpool #L-003126; Dharmacon), siHER3 (ON-TARGETplus, SMARTpool #L-003127; Dharmacon), p44/42 MAPK (ERK1/2) siRNA (Cell Signaling Technology; #6560), AKT1 siRNA (ON-TARGETplus, SMARTpool #L-003000; Dharmacon), c-Jun siRNA (ON-TARGETplus, SMARTpool #L-003268; Dharmacon), or nontargeting siRNA (siNT; ON-TARGETplus Non-targeting Pool, #D-001810; Dharmacon) using Lipofectamine RNAiMAX according to the manufacturer's instructions (Life Technologies).

### Immunoblot analysis

Whole-cell lysis was performed as previously described (31, 33). Enhanced chemiluminescence (ECL) detection system was used to visualize proteins. For detection of phosphorylated AXL, cells were treated with pervanadate (0.12 mmol/L Na<sub>3</sub>VO<sub>4</sub> in 0.002% H<sub>2</sub>O<sub>2</sub>) for 2 minutes before cell lysis, a method previously described (10). EGF and TGF $\alpha$  ligands were added to growth media 45 minutes before lysis.

### Immunoprecipitation

Cells were processed for immunoprecipitation as previously described (34). Five-hundred micrograms of protein, 2  $\mu$ g of anti-AXL (Santa Cruz Biotechnology), cetuximab, or IgG antibody (Santa Cruz Biotechnology) were used.

### Cell proliferation assay

Crystal violet assay and Cell Counting Kit-8 (Dojindo Molecular Technologies) were performed as previously described (31, 35). Cellular proliferation was measured 72 hours after siRNA or drug treatment.

### Flow cytometric analysis

Cells were processed as previously described (36) and analyzed using a FACSCalibur flow cytometer (BD Biosciences). Propidium iodide was added to each sample at a final concentration of 5 mg/mL. Histogram analysis was performed using FlowJo software (TreeStar Inc.).

### Plasmids, transfection, and stable cell line construction

pDONR223-AXL (Plasmid 23945) was purchased from Addgene and subcloned into the *Bam*H1/*Eco*R1 restriction sites of the pcDNA6.0 expression vector (Life Technologies). Stable transfection was performed using Lipofectamine LTX and Opti-MEM I (Life Technology) commencing 48 hours after transfection via 6  $\mu$ g/mL blasticidin to the growth media. Single-cell clones were chosen for expansion and validation for AXL expression.

### cDNA synthesis and qPCR

Total RNA and cDNA synthesis were prepared as previously described (34). All reactions were performed in triplicate. To determine the normalized value,  $2^{\Delta\Delta C_t}$  values were compared between AXL and 18S, where the change in crossing threshold ( $\Delta C_t$ ) =  $C_{t\text{ AXL}} - C_{t\text{ 18S}}$  and  $\Delta\Delta C_t = \Delta C_{t(\text{HC1, HC4, or HC8})} - \Delta C_{t(\text{HP})}$  or  $\Delta\Delta C_t = \Delta C_{t(\text{NT})} - \Delta C_{t(\text{siAXL})}$ .

### Cetuximab-resistant cell line xenografts and PDXs

Ctx<sup>R</sup> cell line xenografts were established as previously described (31), and HNSCC PDXs were established and evaluated for cetuximab response as described in Supplementary Materials and Methods.

### Statistical analysis

Student *t* tests were used to evaluate differences in proliferation, AXL mRNA expression, and pAXL-Y779 expression levels by IHC. Differences were considered statistically significant if \*,  $P < 0.05$ .

## Results

### AXL is overexpressed and activated in a model of acquired resistance to cetuximab

The NSCLC Ctx<sup>R</sup> clones HC1, HC4, and HC8 have been previously shown to be resistant to increasing doses of cetuximab as compared to the Ctx<sup>S</sup> NCI-H226 parental cell line HP (30, 31). Analysis of Ctx<sup>R</sup> clones HC1, HC4, and HC8 demonstrated that all clones expressed increased AXL mRNA and protein as compared to HP cells (Fig. 1A). Furthermore, AXL exhibited increased phosphorylation on tyrosine 702 and 779 in all Ctx<sup>R</sup> clones. In addition, MAPK and AKT pathways were hyperactivated and there was increased expression and phosphorylation of the transcription factor c-Jun in Ctx<sup>R</sup> clones. Moreover, plasma membrane levels of AXL were detected via flow cytometry, where Ctx<sup>R</sup> cells had approximately 50% to 80% more surface AXL expression as compared to HP cells (Fig. 1B). Collectively, these data demonstrate that AXL is overexpressed and activated in established clones with acquired resistance to cetuximab.

### AXL and EGFR cooperate in Ctx<sup>R</sup> clones to sustain proliferation via MAPK and c-Jun

Ctx<sup>R</sup> clones are known to be highly dependent on EGFR for proliferation (30–32). To determine whether AXL also plays a role in Ctx<sup>R</sup> cell proliferation, proliferation assays were

performed 72 hours after transfection with a pooled siAXL or siNT (Fig. 2A). Loss of AXL expression resulted in statistically significant inhibition of proliferation (25%–35%) in all three Ctx<sup>R</sup> clones. As compared with parental HP cells, the Ctx<sup>R</sup> clones demonstrated significantly greater decreases in proliferation after AXL knockdown ( $P < 0.01$ ). Analysis of Ctx<sup>R</sup> clones after AXL knockdown demonstrated that EGFR activation was severely diminished at both tyrosine 1068 and 1173, autophosphorylation sites responsible for recruiting Grb2 and Shc (Fig. 2B; ref. 37). In addition, the activation of c-Raf, p44/42 MAPK, AKT, and ribosomal protein S6 (rpS6) were diminished in all Ctx<sup>R</sup> clones upon AXL knockdown, whereas the activation of these molecules were relatively unchanged or slightly increased in HP cells (Fig. 2B). Interestingly, ablation of HER2 or HER3 receptors, previously shown to be hyperactivated in Ctx<sup>R</sup> cells (30), did not affect the phosphorylation of EGFR at either tyrosine site (Fig. 2B, inset). Collectively, these data demonstrate that Ctx<sup>R</sup> clones are dependent on AXL for cellular proliferation via EGFR activation and downstream signaling.

To determine whether AXL and EGFR were physically associated in Ctx<sup>R</sup> clones, coimmunoprecipitation experiments were performed and indicated that AXL was associated with EGFR in all Ctx<sup>R</sup> clones but not parental cells (Fig. 2C). EGFR and AXL cooperation was further analyzed by reciprocally knocking down EGFR expression with siRNA (Fig. 2D). EGFR knockdown

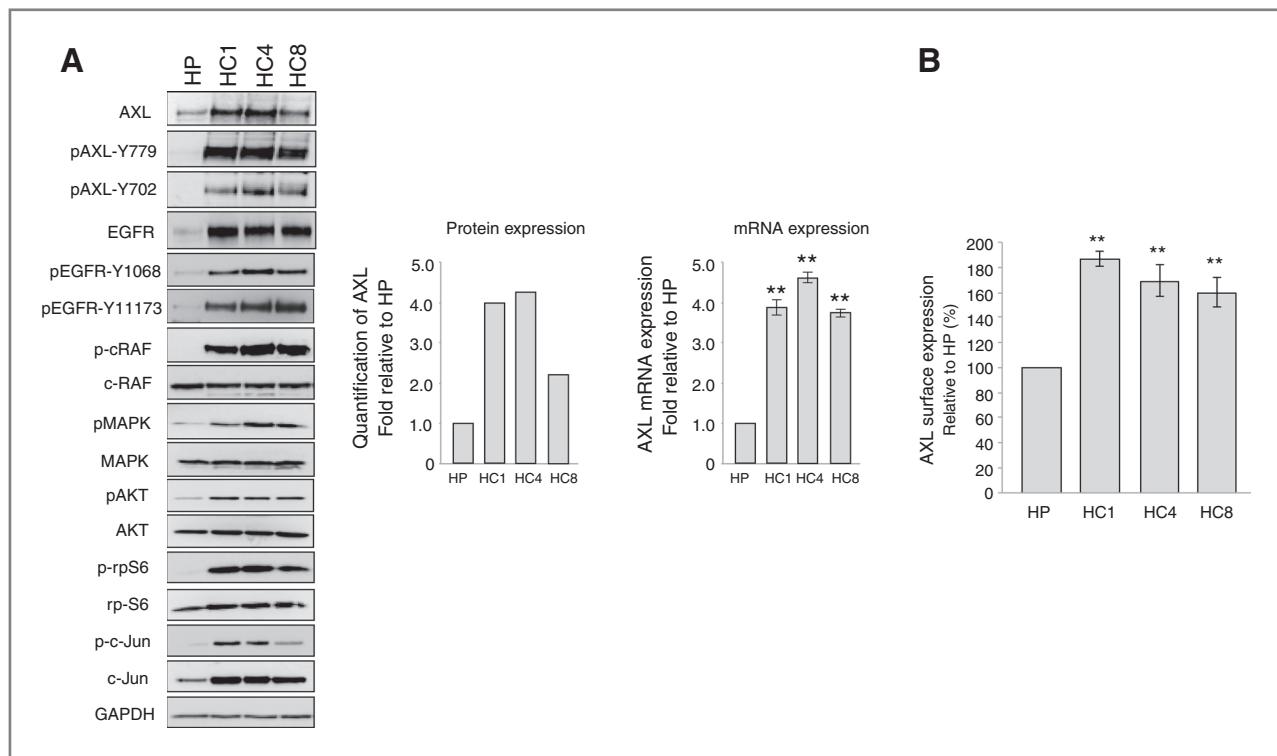


**Figure 1.** The RTK AXL and its downstream effector molecules are overexpressed in cetuximab resistant cells. A, whole-cell lysate was harvested from the Ctx<sup>S</sup> parental cell line (HP) and three Ctx<sup>R</sup> cell clones (HC1, HC4, and HC8) followed by immunoblotting for the indicated proteins. GAPDH was used as a loading control. Total AXL protein expression was quantitated using ImageJ software. AXL mRNA expression was detected by qPCR and normalized to AXL expression in HP cells ( $n = 3$  in three independent experiments). 18S was used as an endogenous control. B, surface level AXL expression was detected by flow cytometry and normalized to HP. IgG-stained cells were used as a background control ( $n = 3$  in two independent experiments). Data, mean  $\pm$  SEM. \*\*,  $P < 0.01$ .



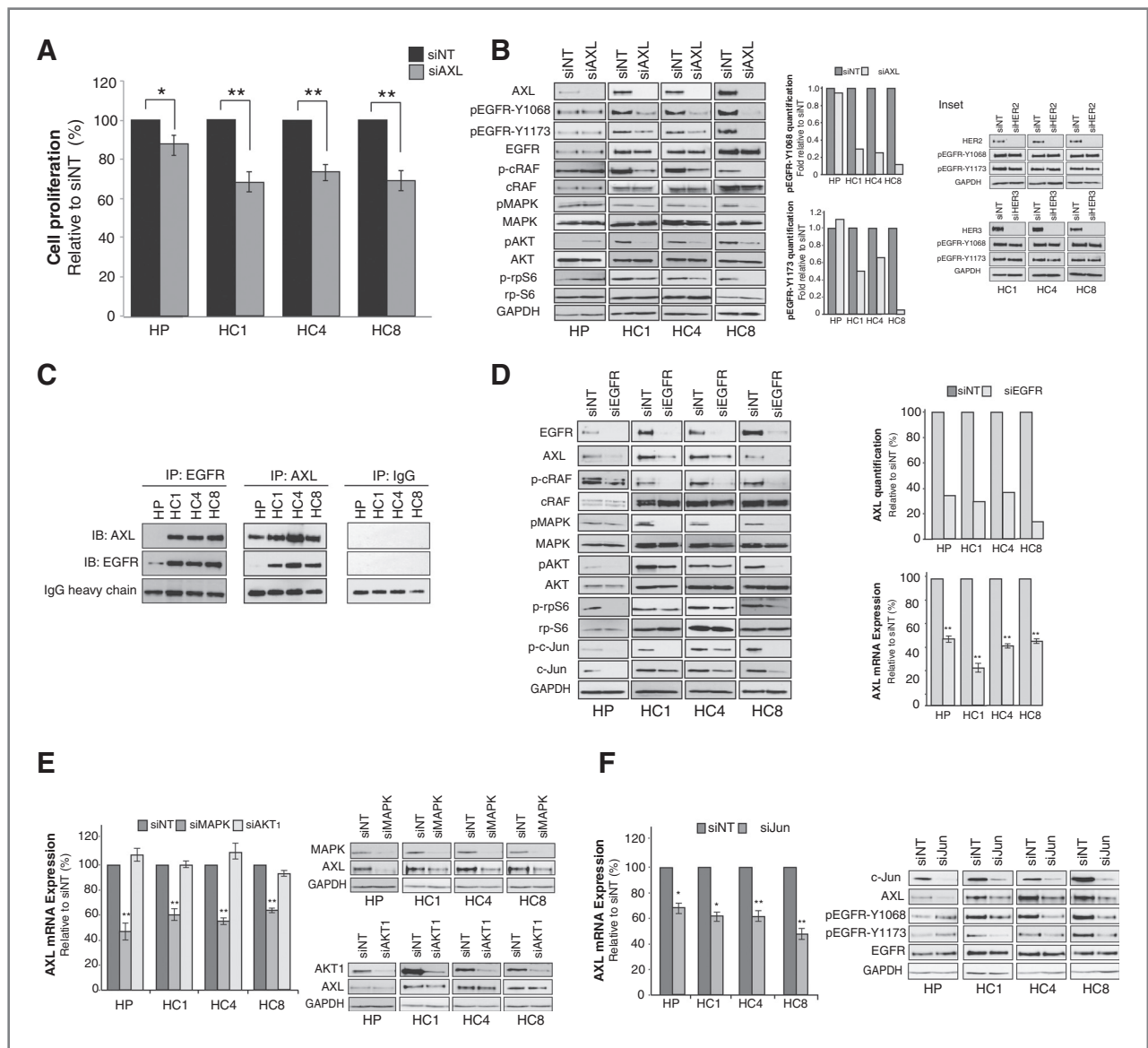


**Figure 2.** Cetuximab-resistant cells depend on AXL and its cooperation with EGFR. **A**, cells were transfected with siAXL or siNT for 72 hours before performing proliferation assays. Proliferation is plotted as percentage of growth relative to NT-transfected cells ( $n = 6$  in three independent experiments). **B**, cells were incubated with siAXL or NT siRNA for 72 hours before harvesting whole-cell lysate and immunoblotting for the indicated proteins. GAPDH was used as a loading control. Phosphorylation of EGFR on tyrosine 1068 and 1173 were quantitated using ImageJ software. Inset, cells were transfected with siRNA against HER2, HER3, or NT siRNA for 72 hours before harvesting whole-cell lysate. GAPDH was used as a loading control. **C**, 500  $\mu$ g of whole-cell lysate was subjected to immunoprecipitation (IP) analysis with cetuximab (IP:EGFR), anti-AXL (IP:AXL), or anti-IgG (IP:IgG) antibody followed by immunoblotting (IB) for EGFR. IgG heavy chain staining from the IB:AXL blot was used as a loading control. **D–F**, whole-cell lysate and mRNA were harvested from Ctx<sup>R</sup> clones 72 hours after transfection with EGFR siRNA (**D**), MAPK and AKT1 siRNAs (**E**), c-Jun siRNA (**F**), or NT siRNA. GAPDH was used as loading control for protein. In **D**, AXL protein expression was quantitated using ImageJ software. AXL mRNA expression was detected by qPCR and normalized to AXL expression in siNT-transfected cells ( $n = 3$  in three independent experiments). 18S was used as an endogenous control. Data, mean  $\pm$  SEM. \*,  $P < 0.05$ ; \*\*,  $P < 0.01$ .

led to a loss of total AXL protein and mRNA expression in Ctx<sup>R</sup> clones and parental HP cells, as well as diminished activation of c-Raf, p44/42 MAPK, AKT, rpS6, and c-Jun. To examine whether EGFR regulation of AXL was contingent on MAPK or AKT signaling directly, we alternatively knocked down p44/42 MAPK or AKT1 with siRNA (Fig. 2E). This experiment indicated that knockdown of p44/42 MAPK led to a loss of AXL mRNA and

protein expression, whereas AKT1 did not regulate AXL expression. These results suggest that EGFR regulates AXL expression specifically through MAPK signaling.

Previous studies indicated that the AXL promoter contains binding motifs for AP-1 family transcription factors, in which phorbol myristate acetate (PMA) stimulation of leukemia cells led to increased AXL expression through MAPK signaling to

the transcription factor c-Jun (38). Because Ctx<sup>R</sup> clones were found to overexpress c-Jun (Fig. 1A), we hypothesized that c-Jun may function downstream of MAPK to regulate AXL mRNA expression. To investigate this, c-Jun was knocked down with siRNA (Fig. 2F), leading to an approximate 35% to 55% decrease in AXL mRNA levels. Moreover, there was a loss of AXL protein expression, which appeared similar to the levels detected after EGFR or MAPK knockdown (Fig. 2D and E). Importantly, this led to a loss of EGFR activation in Ctx<sup>R</sup> clones, but not in parental HP cells, indicating that AXL is required for EGFR activation and subsequent signaling in the resistant setting. Collectively, these data indicate that AXL expression and subsequent EGFR activation are regulated through the MAPK/c-Jun signaling pathway in Ctx<sup>R</sup> clones.

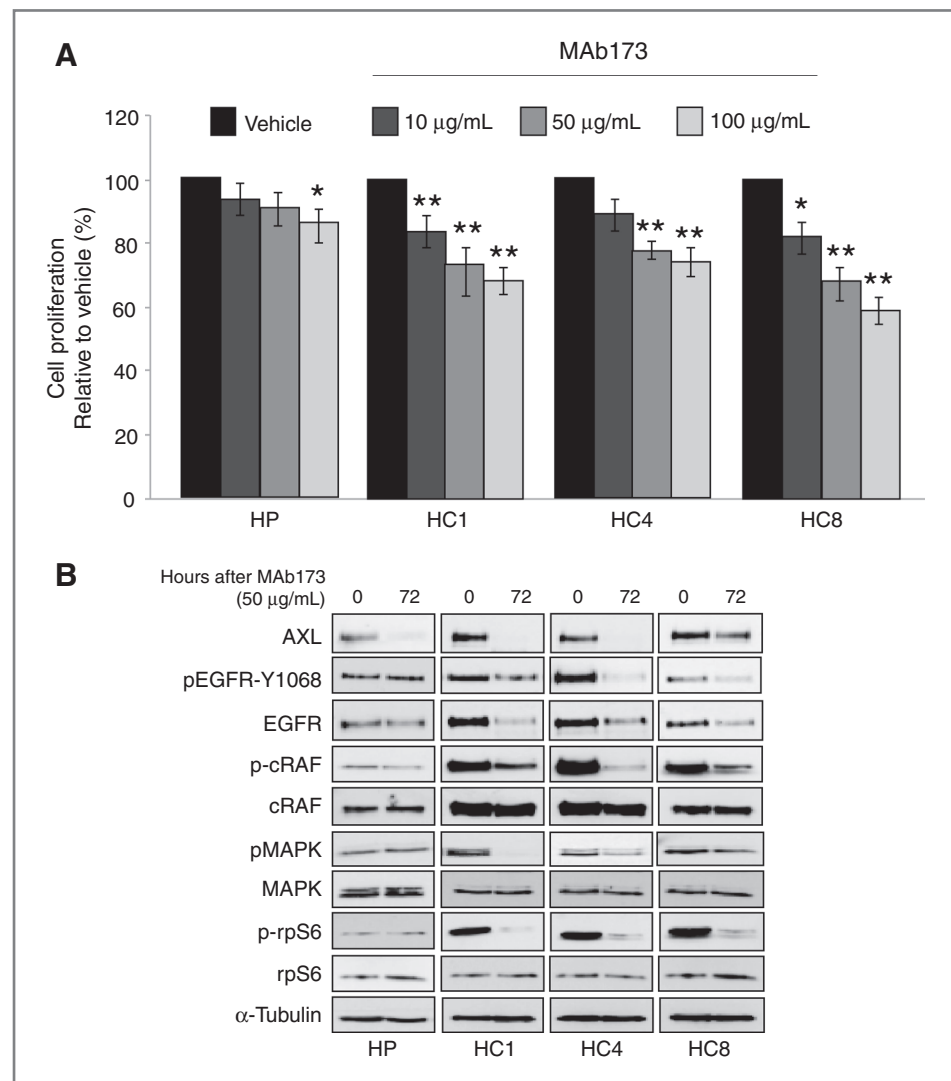
### Ctx<sup>R</sup> cells are sensitive to anti-AXL monoclonal antibody and TKI therapies

Because Ctx<sup>R</sup> clones were sensitive to AXL knockdown by siRNA, we hypothesized that these cells would also be sensitive

to anti-AXL therapeutics. First, we tested the ability for the anti-AXL monoclonal antibody MAb173 to inhibit Ctx<sup>R</sup> cell proliferation (Fig. 3A). Ctx<sup>R</sup> clones were significantly growth inhibited upon treatment with increasing doses of MAb173, whereas Ctx<sup>S</sup> HP cells were less sensitive. In addition, the growth-inhibitory effects of Ctx<sup>R</sup> clones were statistically decreased from the effect on HP cells when treated with 50 and 100  $\mu\text{g/mL}$  of MAb173 ( $P < 0.01$ ). Consistent with previous studies (9), MAb173 induced AXL degradation (Fig. 3B). Interestingly, total EGFR protein levels were reduced upon MAb173 treatment of Ctx<sup>R</sup> clones, in addition to loss of MAPK signaling. MAb173 did not affect the activation of EGFR or MAPK signaling in HP cells.

Next, the small-molecule TKI R428, which has greater than 100-fold selectivity for AXL as compared with EGFR or Tyro and 50-fold greater affinity than Mer (39), was tested for therapeutic benefit in Ctx<sup>R</sup> clones (Fig. 4A). All Ctx<sup>R</sup> clones demonstrated robust antiproliferative effects upon treatment with 0.8 and 1  $\mu\text{mol/L}$  of R428, whereas HP cells were less

**Figure 3.** Cetuximab-resistant cells are sensitive to therapeutic degradation of AXL with the monoclonal antibody MAb173. A, cells were subjected to increasing doses of MAb173 (10, 50, and 100  $\mu\text{g/mL}$ ) for 72 hours before performing proliferation assays. Proliferation is plotted as a percentage of growth relative to vehicle treated cells ( $n = 6$  in three independent experiments). Data, mean  $\pm$  SEM. \*,  $P < 0.05$ ; \*\*,  $P < 0.01$ . B, cells were subjected to 50  $\mu\text{g/mL}$  of MAb173 for 72 hours before harvesting whole-cell lysate and immunoblotting for the indicated proteins.  $\alpha$ -Tubulin was used as a loading control.



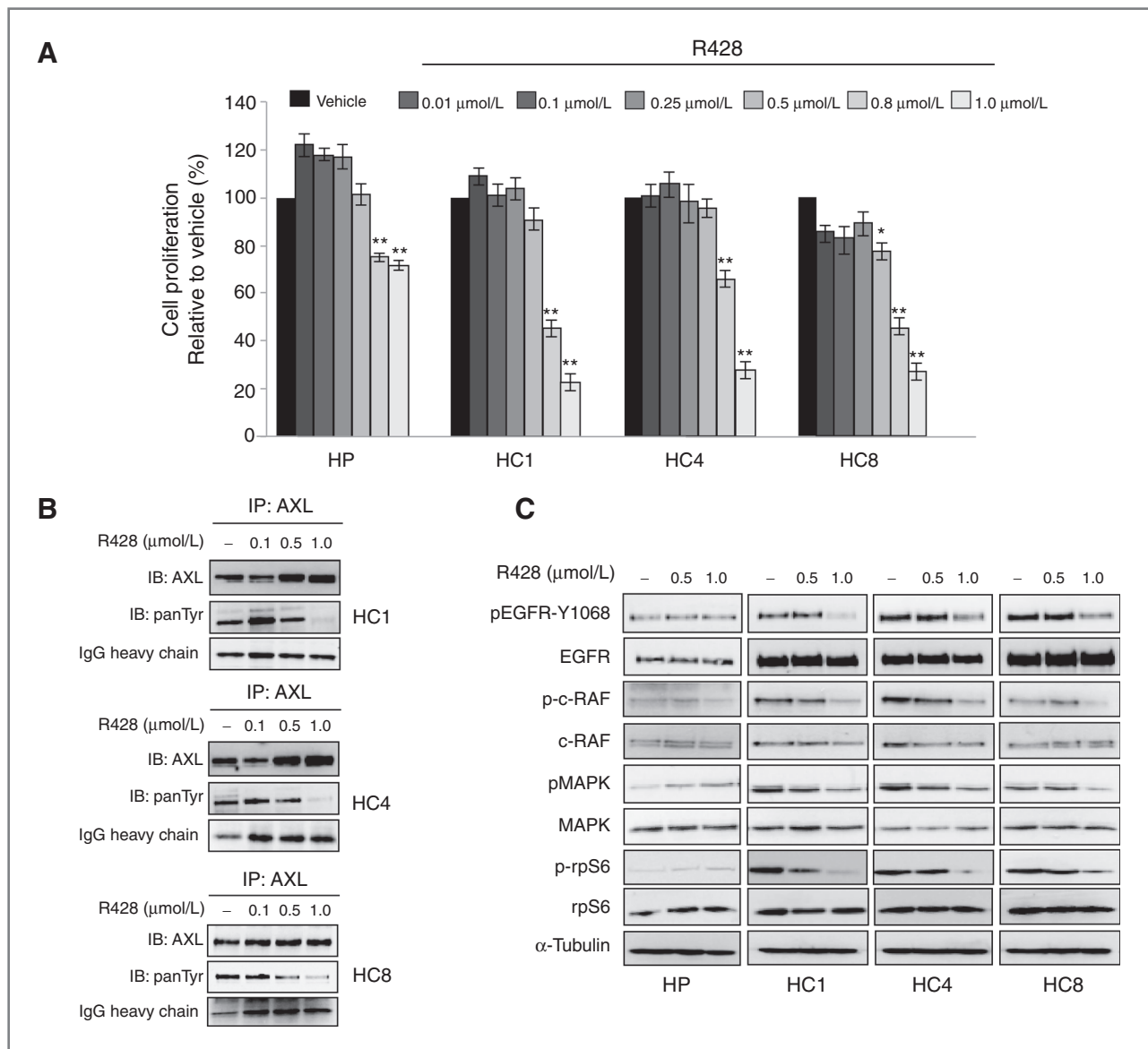


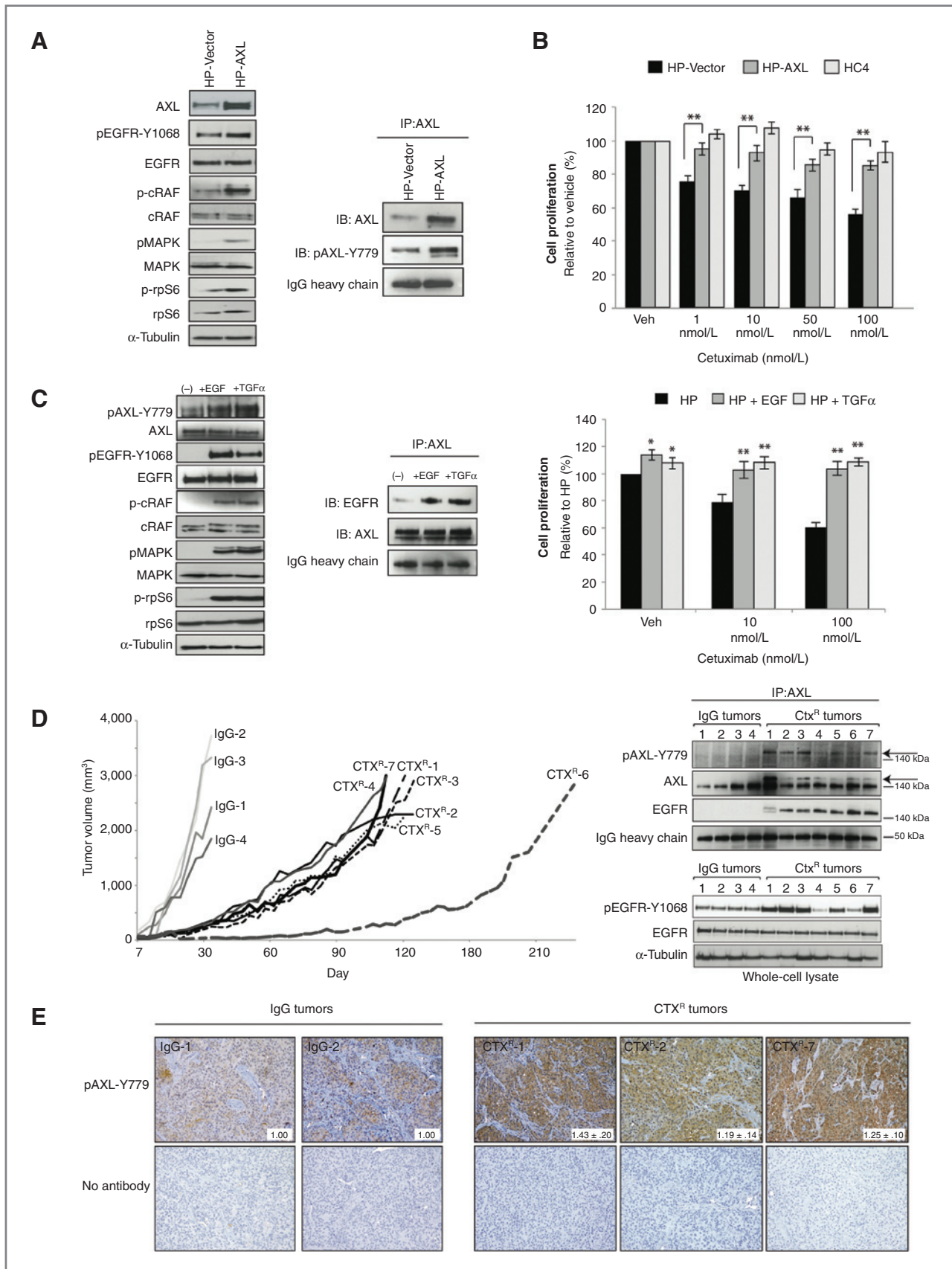
**Figure 4.** Cetuximab-resistant cells are sensitive to therapeutic blockade of AXL activity with the AXL TKI R428. **A**, cells were subjected to increasing doses of R428 (0.01–1 μmol/L) for 72 hours before performing proliferation assays. Proliferation is plotted as a percentage of growth relative to vehicle-treated cells ( $n = 6$  in four independent experiments). Data, mean  $\pm$  SEM. \*,  $P < 0.05$ ; \*\*,  $P < 0.01$ . **B**, cells were treated with vehicle (–) or indicated doses of R428 for 24 hours. 500 μg of whole-cell lysate was subjected to immunoprecipitation analysis with an anti-AXL antibody followed by immunoblotting for either AXL or pan-tyrosine (panTyr). IgG heavy chain staining from the IB:AXL blot was used as a loading control. **C**, cells were treated with vehicle (–) or indicated doses of R428 for 24 hours before harvesting whole-cell lysate and immunoblotting for the indicated proteins.  $\alpha$ -Tubulin was used as a loading control.

sensitive at these concentrations. In addition, the growth-inhibitory effects of Ctx<sup>R</sup> clones were statistically decreased from the effect on HP cells when treated with 0.8 and 1 μmol/L of R428 ( $P < 0.01$ ). Analysis of Ctx<sup>R</sup> clones after treatment, via pan-tyrosine, demonstrated that AXL phosphorylation was inhibited with 1.0 μmol/L of R428, the same dose that elicited antiproliferative responses (Fig. 4B). In addition, R428 treatment led to a loss of EGFR phosphorylation on tyrosine 1068 and MAPK signaling, whereas these targets were relatively unaffected in HP cells (Fig. 4C). Interestingly, both MAb173 and

R428 did not influence the apoptosis pathway in Ctx<sup>R</sup> clones (data not shown), indicating that AXL more predominantly activates growth-promoting pathways in resistant cells.

#### AXL activation and overexpression confers cetuximab resistance *in vitro* and *in vivo* mouse xenograft models

To confirm the role of AXL in cetuximab resistance, AXL was stably overexpressed in the Ctx<sup>S</sup> parental cell line HP (Fig. 5A). Immunoprecipitation analysis of HP-AXL stable cells indicated that AXL was phosphorylated on tyrosine 779, resulting in





increased phosphorylation of EGFR and downstream MAPK signaling. Cetuximab dose–response proliferation assays demonstrated that HP-AXL cells were statistically more resistant to cetuximab as compared with HP-Vector cells ( $P < 0.01$ ; Fig. 5B). HC4 cells served as a cetuximab-resistant control in these experiments. These data demonstrate that the stable overexpression of AXL can confer resistance to cetuximab in a Ctx<sup>S</sup> cell line, supporting a putative role for AXL in the development of cetuximab resistance.

We previously reported that Ctx<sup>R</sup> clones overexpressed EGFR ligands (36); however, whether EGFR ligands influenced cetuximab resistance through regulating AXL activity and/or association with the EGFR was not investigated. Therefore, HP cells were stimulated with two EGFR ligands, EGF or TGF $\alpha$ , and subsequently measured for AXL activation, association with the EGFR, and cetuximab response (Fig. 5C). Analysis of HP cells after ligand stimulation indicated that both ligands led to increased AXL activation and association with the EGFR (detected by immunoprecipitation analysis). In addition, incubation with either ligand resulted in increased resistance to cetuximab. Interestingly, the ligand for AXL, Gas6, was not overexpressed in Ctx<sup>R</sup> clones and did not drive resistance in HP cells (data not shown). Collectively, these data suggest that EGFR ligands may influence cetuximab resistance through stimulating AXL activation and association with the EGFR.

To further analyze the role of AXL in cetuximab resistance, we developed *de novo* tumors with acquired resistance to cetuximab *in vivo* (31, 32). To develop *de novo*–acquired resistance, the Ctx<sup>S</sup> cell line NCI-H226 was inoculated unilaterally into the dorsal flank of 11 athymic nude mice (Fig. 5D). Once tumors reached approximately 100 mm<sup>3</sup>, 4 mice were treated with IgG control antibody (1 mg/mouse) and 7 mice were treated with cetuximab (1 mg/mouse) by intraperitoneal injection twice weekly. Tumors treated with IgG grew rapidly (tumors denoted as IgG-1 to IgG-4 in Fig. 5D), whereas all cetuximab-treated tumors displayed initial growth control. Acquired resistance was observed after approximately 30 days of cetuximab exposure in 6 of the cetuximab-treated mice (tumors denoted as Ctx<sup>R</sup>-1 to Ctx<sup>R</sup>-5, and Ctx<sup>R</sup>-7), at which point there was marked tumor growth in the presence of continued cetuximab therapy (Fig. 5D). One mouse was continued on cetuximab for 90 days until a significant increase in tumor growth was observed (Ctx<sup>R</sup>-6). Once tumors reached

2,000 mm<sup>3</sup>, they were harvested and processed for immunoblot analysis (Fig. 5D) and IHC (Fig. 5E). To detect the levels of total and activated AXL (Y779), immunoprecipitation analysis was performed from tumor lysates. Strikingly, a double banding pattern for total AXL was observed in all Ctx<sup>R</sup> tumors, whereas a single AXL band was observed in the IgG-treated tumors. The upper band corresponds to a shift in AXL molecular weight due to the presence of phosphorylated AXL, which was detected by the phospho AXL-Y779 antibody (Fig. 5D, arrows). In addition, AXL was associated with EGFR only in the Ctx<sup>R</sup> tumors by immunoprecipitation (Fig. 5D). Analysis of whole-cell lysate indicated that EGFR was also highly activated (indicated by tyrosine 1068 phosphorylation) in the Ctx<sup>R</sup> tumors that expressed the highest levels of pAXL-Y779. IHC analysis of IgG versus Ctx<sup>R</sup> tumors revealed that Ctx<sup>R</sup> tumors had statistically significant increases in pAXL-Y779 staining (Fig. 5E). Collectively, these data demonstrate that AXL overexpression and/or activation plays a role in acquired resistance to cetuximab *in vitro* and *in vivo*.

To expand these findings to a more clinically relevant model system, we determined whether there was a correlation between cetuximab response and AXL expression in PDXs established directly from surgically resected HNSCCs. Six PDXs were established from patients who had not received prior cetuximab therapy (see Supplementary Table S1 for clinical characteristics of patients before surgery). For each PDX, dual flank tumors were established in 16 athymic nude mice. When tumors reached approximately 200 mm<sup>3</sup>, the mice were stratified into two treatment groups: control (vehicle-treated) and cetuximab ( $n = 8$  mice/16 tumors per group). After completing the treatment regimen, tumor growth was monitored to evaluate response to therapy. Overall, there were three cetuximab-sensitive PDXs (UW-SCC36, UW-SCC22, and UW-SCC52) and three cetuximab-resistant PDXs (UW-SCC1, UW-SCC17, and UW-SCC25; Fig. 6).

PDXs harvested from early-passaged tumors before treatment were evaluated for AXL expression and activation by IHC analysis (Fig. 6). The cetuximab-sensitive PDXs had low levels of AXL and pAXL-Y779 staining, with UW-SCC36 having nearly absent expression of both markers. In comparison, the three cetuximab-resistant PDXs expressed 1.8- to 2.5-fold increases in pAXL-Y779 expression, and 2.5- to 4.3-fold increases in total AXL expression as compared with the staining intensity

**Figure 5.** AXL overexpression and activity results in cetuximab resistance in Ctx<sup>S</sup> cells *in vitro* and in *de novo* models of Ctx<sup>R</sup> *in vivo*. A, HP cells were made to stably express either pcDNA6.0-AXL (HP-AXL) or pcDNA6.0-Vector (HP-Vector). Whole-cell lysate was harvested and subjected to immunoblot analysis.  $\alpha$ -Tubulin was used as a loading control. 500  $\mu$ g of protein was subjected to immunoprecipitation with an anti-AXL antibody for analysis of pAXL-Y779. IgG heavy chain staining from the IB:AXL blot was used as a loading control. B, HP-AXL, HP-Vector, or HC4 cells were treated with increasing doses of cetuximab (1–100 nmol/L) for 72 hours before performing proliferation assays. Proliferation is plotted as a percentage of growth relative to vehicle treated cells ( $n = 6$  for four independent experiments). Data, mean  $\pm$  SEM. \*\*,  $P < 0.01$ . C, HP cells were stimulated with 50 ng/mL of EGF or TGF $\alpha$  for 45 minutes before harvesting whole-cell lysate. Of note, 500  $\mu$ g of protein was subjected to immunoprecipitation with an anti-AXL antibody for analysis of EGFR association. Proliferation assays were performed 72 hours after treatment with increasing doses of cetuximab and either 50 ng/mL EGF or TGF $\alpha$ . Proliferation is plotted as a percentage of growth relative to vehicle-treated HP cells ( $n = 8$  for three independent experiments). Data, mean  $\pm$  SEM. \*,  $P < 0.05$ ; \*\*,  $P < 0.01$ . D and E, established Ctx<sup>S</sup> NCI-H226 xenografts were treated with cetuximab (1 mg/mouse) or IgG twice weekly. IgG-treated tumors grew uninhibited (IgG-1–IgG-4), whereas acquired resistance to cetuximab was observed after day 30 in 6 of 7 treated mice (Ctx<sup>R</sup>-1 to Ctx<sup>R</sup>-5, and Ctx<sup>R</sup>-7). Ctx<sup>R</sup>-6 acquired resistance after 90 days of treatment. D, 500  $\mu$ g of tumor cell lysate was subjected to immunoprecipitation with an anti-AXL antibody followed by immunoblotting for pAXL-Y779, AXL, or EGFR. IgG heavy chain staining from the IB:AXL blot was used as a loading control. pEGFR-Y1068 status was defined by Western blot analysis.  $\alpha$ -Tubulin was used as a loading control. E, IHC analysis of pAXL-Y779 in tumor samples (20 $\times$ ). Quantitation of IHC was performed via ImageJ software (average of 5 independent fields of view per tumor); values were normalized to the average staining in IgG tumor sections.

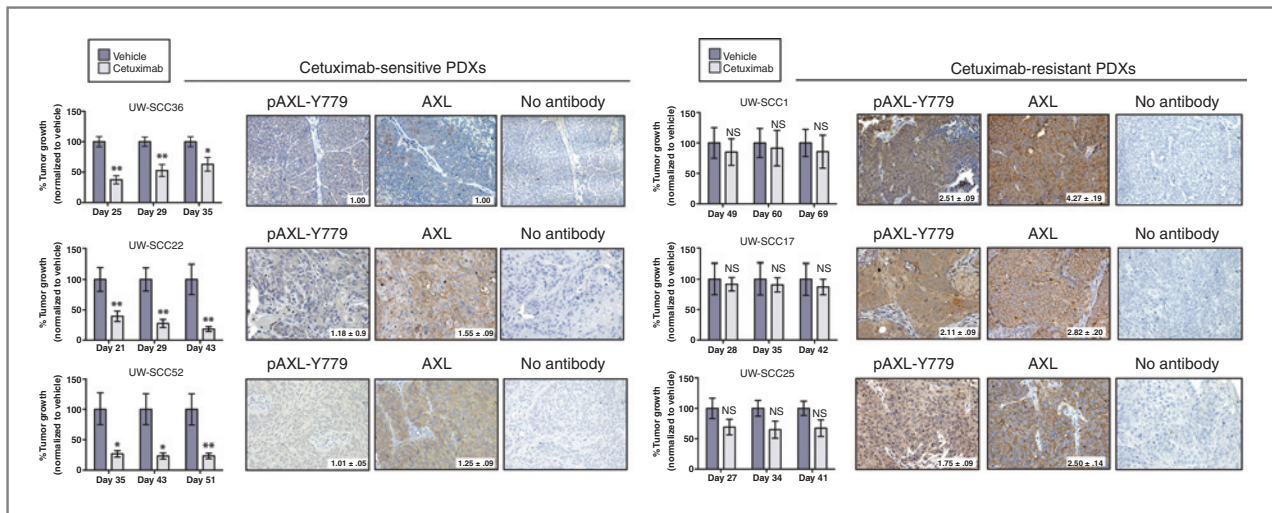


**Figure 6.** AXL is overexpressed and activated in cetuximab-resistant HNSCC PDXs. PDXs were evaluated for cetuximab response as described in Supplementary Materials and Methods. Tumor growth was plotted as a percentage of averaged vehicle treated tumor volumes at the last three time points of the study; \*,  $P < 0.05$ ; \*\*,  $P < 0.01$ . Representative images of IHC analysis of AXL and pAXL-Y779 staining in early-passaged PDXs are shown (20 $\times$ ). Quantitation of IHC was performed via ImageJ software (average of 2–5 independent tumors were stained and imaged); values were normalized to the average staining of UW-SCC36. NS, not significant.

detected in UW-SCC36 tumors. Collectively, these data demonstrate that AXL is overexpressed and activated in PDXs that are intrinsically resistant to cetuximab therapy.

### AXL plays a role in acquired resistance to cetuximab in HNSCC

To further investigate whether AXL plays a more global role in acquired resistance to cetuximab, we developed a model of acquired resistance to cetuximab using the Ctx<sup>S</sup> parental cell line UM-SCC1 (30). This resulted in a parental SCC1 cell line (SP) and three cetuximab-resistant clones (SP7, SP8, and SP11). SP cell growth was inhibited upon treatment with increasing doses of cetuximab, while the three HNSCC Ctx<sup>R</sup> clones remained resistant (Fig. 7A). Analysis of HNSCC Ctx<sup>R</sup> clones indicated that all clones had increased steady-state expression of AXL as compared with SP (Fig. 7B). In addition, each clone demonstrated increased activation of c-Raf, p44/42 MAPK, AKT, rpS6, and c-Jun (Fig. 7B). To determine whether AXL influenced HNSCC Ctx<sup>R</sup> cell proliferation, cells were transfected with siAXL or NT siRNA and proliferation assays were performed. Loss of AXL expression resulted in a significant inhibition in cellular proliferation (20%–25%) in HNSCC Ctx<sup>R</sup> clones, while parental SP cells were nonresponsive (Fig. 7C). The growth-inhibitory effects of siAXL in HNSCC Ctx<sup>R</sup> clones were statistically decreased compared with the effect on SP cells ( $P < 0.01$ ). Furthermore, all HNSCC Ctx<sup>R</sup> clones expressed diminished activation of EGFR (by tyrosine 1068 phosphorylation) as well as MAPK and AKT signaling pathways upon AXL knockdown, whereas the activation of these molecules was relatively unchanged or slightly increased in SP cells. Collectively, these data suggest that AXL plays a role in acquired resistance to cetuximab in HNSCC.

### Discussion

Cetuximab is a commonly used anti-EGFR monoclonal antibody that has demonstrated efficacy in treating in HNSCC, mCRC, and NSCLC (19–26). Although cetuximab treatment has yielded clinical benefit, both intrinsic and acquired resistance are common outcomes. Recently, a novel mutation was identified in the EGFR (S492R) that mediates resistance to cetuximab (40); however, resistance also occurs in the WT setting. Multiple mechanisms of cetuximab resistance exist, including upregulation of EGFR ligands (41), nuclear translocation of EGFR (36), oncogenic shift to vascular endothelial growth factor receptor-1 (VEGFR-1; ref. 42), and constitutive activation of downstream signaling molecules such as KRAS (43) and c-Src (44). This study is the first to describe a role for AXL in mediating cetuximab resistance in the setting of wild type (WT) EGFR, and thus provides rationale for the development and use of anti-AXL therapeutics for treatment of Ctx<sup>R</sup> tumors.

Cetuximab resistance is challenging to study due to the lack of access to patient tissue upon relapse. To model Ctx<sup>R</sup> mechanisms that may occur in humans, several models of acquired resistance were established via prolonged exposure of Ctx<sup>S</sup> cells to cetuximab (30–32). These models indicated that Ctx<sup>R</sup> clones and tumors had increased expression and dependency on the EGFR (30–32). In this study, AXL was found to activate EGFR in Ctx<sup>R</sup> clones, whereas HER2 and HER3 receptors did not, suggesting that AXL is a key mediator of EGFR activity in the resistant setting. Furthermore, EGFR and AXL were associated in Ctx<sup>R</sup> clones and tumors (Figs. 2C and 5D), a finding previously reported in triple-negative breast cancers (TNBC; ref. 14), tumors that are intrinsically resistant to cetuximab. Interestingly, EGF mediated AXL-induced signaling pathways in TNBC, whereas Gas6 did not (14), similar to our findings in Fig. 5C. Another novel finding was that EGFR signaling led to increased AXL mRNA expression in Ctx<sup>R</sup>

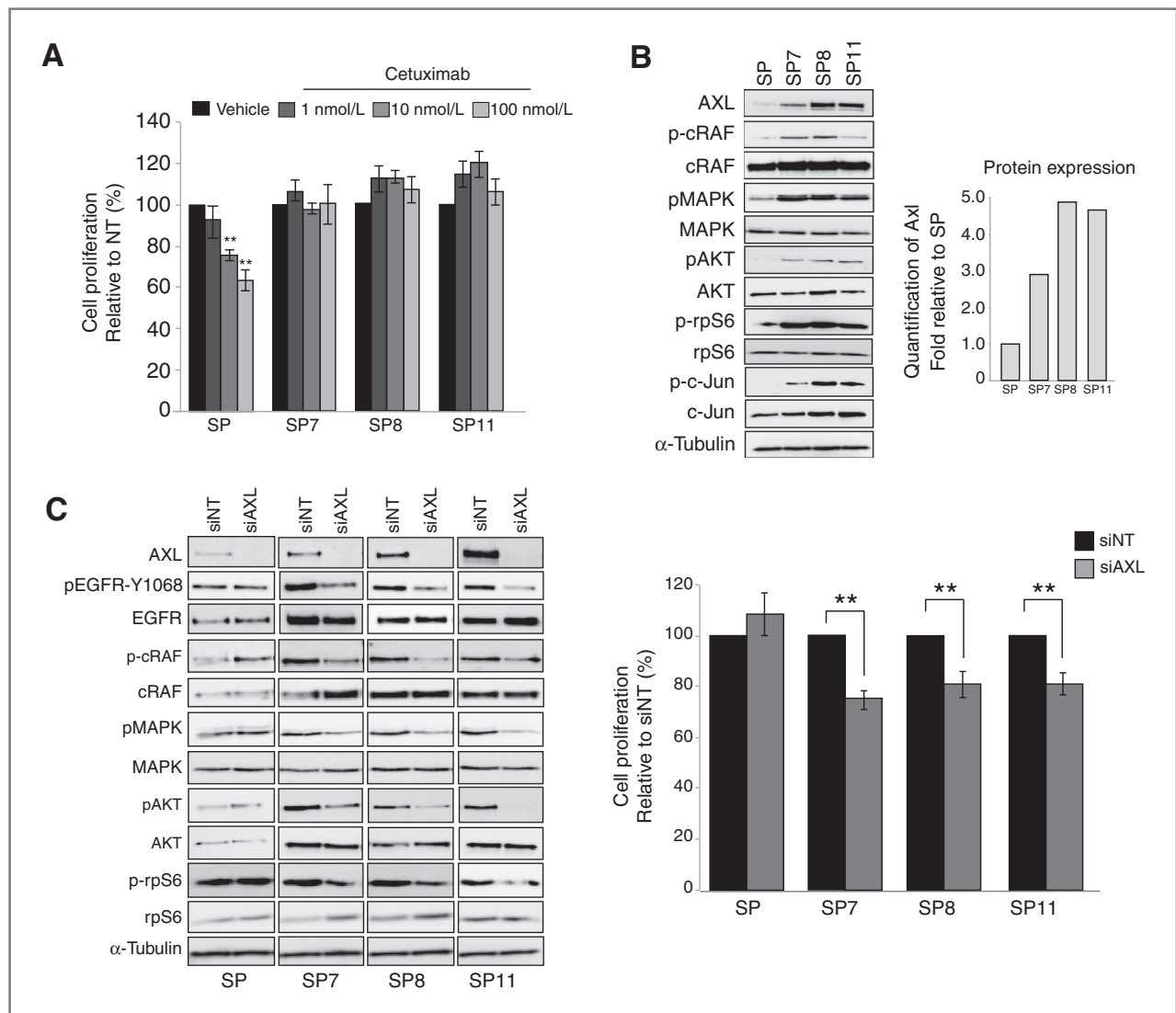


**Figure 7.** AXL mediates acquired resistance to cetuximab in HNSCC. **A**, Ctx<sup>R</sup> cell clones (SP7, SP8, and SP11) and the Ctx<sup>S</sup> parental cell line (SP) were treated with increasing doses of cetuximab (1, 10, and 100 nmol/L) for 72 hours before performing proliferation assays. Proliferation is plotted as a percentage of growth relative to vehicle-treated cells ( $n = 5$  for three independent experiments). **B**, whole-cell lysate was harvested from cells followed by immunoblotting for the indicated proteins.  $\alpha$ -Tubulin was used as a loading control. Total AXL protein expression was quantitated using ImageJ software. **C**, cells were incubated with siAXL or nontargeting (NT) siRNA for 72 hours before performing proliferation assays or isolation of whole-cell lysate and immunoblotting for indicated proteins.  $\alpha$ -Tubulin was used as a loading control. Proliferation is plotted as a percentage of growth relative to NT-transfected cells ( $n = 3$  for three independent experiments). Data, mean  $\pm$  SEM. \*\*,  $P < 0.01$ .

clones. The regulation of AXL mRNA was contingent on MAPK and c-Jun because knockdown of either decreased AXL expression (Fig. 2E and F).

These data support a positive-feedback loop that occurs in EGFR-dependent Ctx<sup>R</sup> cells (Fig. 8). In this model, resistance is characterized by increased EGFR ligand production, dimerization, and transactivation of AXL and EGFR. This interaction results in hyperactivated MAPK/c-Jun signaling, upregulation of AXL mRNA expression, and maintenance of constitutive EGFR activation and cetuximab resistance. The *de novo* Ctx<sup>R</sup> cell line xenografts support this model, as Ctx<sup>R</sup> tumors expressed increased total and activated AXL (especially as compared with IgG-1 and IgG-2). Although c-Jun was capable

of regulating AXL mRNA expression in Ctx<sup>S</sup> parental cells, this regulation did not reduce EGFR activity (Fig. 2F), suggesting that EGFR and AXL are not coupled in Ctx<sup>S</sup> cells.

Because of limited availability of patient tissue after cetuximab failure, the expression status of AXL and pAXL-Y779 was evaluated in intrinsically resistant HNSCC PDXs. PDXs are clinically relevant cancer models because they accurately maintain many aspects of the parental tumor, including its histology, gene expression profile, copy number variance, and metastatic patterns (45, 46). In this study, total and activated AXL were highly overexpressed in HNSCC PDXs that were resistant to cetuximab (Fig. 6). The strong correlation between AXL and cetuximab resistance observed in the PDXs supports



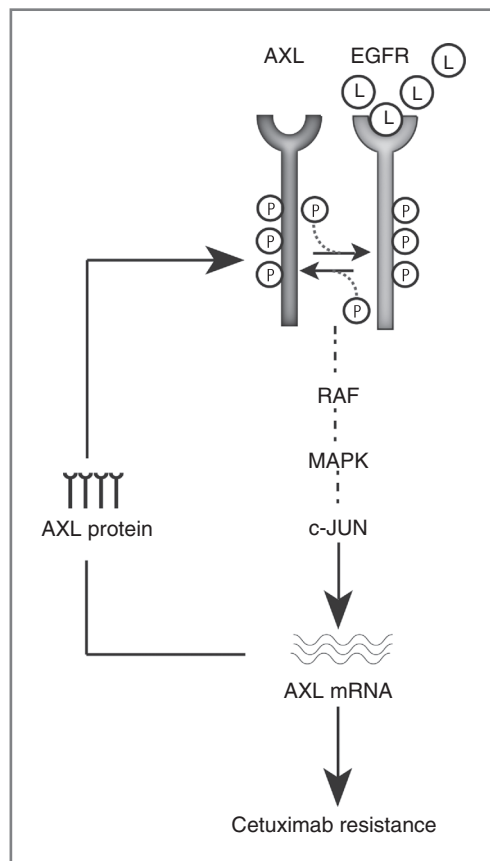


**Figure 8.** Model for AXL and EGFR cooperation in cetuximab resistance. Cetuximab resistance is characterized by increased AXL mRNA and protein expression, EGFR activation, and MAPK pathway signaling. In Ctx<sup>R</sup> cells, increased EGFR ligand (L) production leads to AXL and EGFR association and transactivation. This results in MAPK and c-Jun signaling and subsequent increases in AXL transcription. Increases in AXL mRNA result in elevated AXL protein levels and maintenance of EGFR activation and signaling. This positive feedback loop results in the constitutive activation of both AXL and EGFR in Ctx<sup>R</sup> cells and thereby mediates cetuximab resistance.

the mechanistic work performed in this study and suggests that AXL may mediate both intrinsic and acquired resistance to cetuximab.

To date, AXL has been identified to play a role in resistance to EGFR TKIs in NSCLC (16), HNSCC (13), and TNBC (14). In NSCLC, AXL was overexpressed and activated in EGFR-mutant erlotinib-resistant cells, where AXL inhibition resensitized tumor cells to erlotinib (13, 16). In this study, AXL inhibition was sufficient to inhibit the growth of Ctx<sup>R</sup> clones, but did not resensitize Ctx<sup>R</sup> clones to cetuximab (data not shown). This likely occurred because AXL inhibition robustly decreased EGFR activation; thus, adding cetuximab provided no further benefit. Although AXL inhibition led to robust antiproliferative effects in Ctx<sup>R</sup> clones, cell growth was not completely arrested, suggesting that other RTKs may influence resistance. Previous work from our laboratory and others suggests that signaling emanating from HER2:HER3 heterodimers play a role in resistance to anti-EGFR agents (30, 47). Thus, targeting AXL

and either HER2 or HER3 may result in even more robust antiproliferative responses because EGFR signaling could be abrogated through AXL inhibition and HER2:HER3 signaling could be blocked with anti-HER2 or HER3 agents. Ultimately, this approach may lead to a complete loss of HER family signaling capabilities and serve as a powerful strategy for the treatment of Ctx<sup>R</sup> cancers.

With increasing evidence supporting the role of AXL in resistance to anti-EGFR agents, the development of anti-AXL therapeutics is essential. In this study, two novel anti-AXL therapeutics were tested: MAb173, an anti-AXL-neutralizing monoclonal antibody, and R428, a selective small-molecule AXL TKI. In previous studies, researchers demonstrated that AXL was hyperactivated in Kaposi sarcoma and that MAb173 induced AXL endocytosis and degradation (9). In addition to AXL, total EGFR expression was decreased upon MAb173 treatment of Ctx<sup>R</sup> cells (Fig. 3B), supporting the existence of AXL and EGFR heterodimers and the utility of this antibody in the setting of cetuximab resistance. Furthermore, EGFR was not degraded in MAb173-treated HP cells, which lack AXL and EGFR association (Fig. 2C). The anti-AXL TKI R428 has also shown antitumorigenic effects in multiple cancer models, including breast cancer (14, 39) and HNSCC (13). The differences in growth inhibition observed between MAb173 and R428 may result from off-target effects of R428, leading to more robust antiproliferative responses. R428 has now entered phase I clinical trials, whereas MAb173 is still undergoing preclinical testing.

Overall, AXL plays a key role in tumor growth, metastasis, angiogenesis, and resistance to anti-EGFR agents (12–17). In addition, AXL inhibition has been shown to enhance the efficacy of standard chemotherapy regimens (10, 15, 18). With AXL at the forefront, Tyro and Mer receptors also influence parameters of tumor biology (1, 4). In fact, both Tyro and Mer receptors were differentially overexpressed in the current Ctx<sup>R</sup> models (unpublished data), promoting further research on the global role of TAM receptors in cetuximab resistance. Collectively, the studies herein have strong potential for translation into future clinical trials and therapies for patients with cetuximab-resistant tumors.

### Disclosure of Potential Conflicts of Interest

P.S. Gill is CSO of Vasgene Therapeutics and has ownership interest (including patents) in the same. No potential conflicts of interest were disclosed by the other authors.

### Authors' Contributions

**Conception and design:** T.M. Brand, M. Toulany, P.S. Gill, R. Salgia, D.L. Wheeler

**Development of methodology:** T.M. Brand, M. Iida, A.P. Stein, P.S. Gill, R. Salgia, D.L. Wheeler

**Acquisition of data (provided animals, acquired and managed patients, provided facilities, etc.):** T.M. Brand, A.P. Stein, K.L. Corrigan, C. Braverman, N. Luthar, R. Salgia

**Analysis and interpretation of data (e.g., statistical analysis, biostatistics, computational analysis):** T.M. Brand, M. Iida, A.P. Stein, M. Toulany, K.L. Corrigan, R. Salgia, R.J. Kimple, D.L. Wheeler

**Writing, review, and/or revision of the manuscript:** T.M. Brand, M. Iida, A.P. Stein, K.L. Corrigan, M. Toulany, P.S. Gill, R. Salgia, R.J. Kimple, D.L. Wheeler

**Administrative, technical, or material support (i.e., reporting or organizing data, constructing databases):** T.M. Brand, M. Iida, D.L. Wheeler

**Study supervision:** T.M. Brand, R. Salgia, R.J. Kimple, D.L. Wheeler

## Grant Support

This study was supported by grant UL1TR000427 from the Clinical and Translational Science Award program (to D.L. Wheeler), through the NIH National Center for Advancing Translational Sciences, grant RSG-10-193-01-TBG from the American Cancer Society (to D.L. Wheeler), grant W81XWH-12-1-0467 from United States Army Medical Research and Materiel Command (to D.L. Wheeler), University of Wisconsin Carbone Cancer Center Cancer Center

Support Grant P30 CA014520 (to D.L. Wheeler) and Mary Kay Foundation grant MSN152261 (to D.L. Wheeler).

The costs of publication of this article were defrayed in part by the payment of page charges. This article must therefore be hereby marked *advertisement* in accordance with 18 U.S.C. Section 1734 solely to indicate this fact.

Received February 5, 2014; revised June 11, 2014; accepted June 30, 2014; published OnlineFirst August 18, 2014.

## References

- Linger RM, Keating AK, Earp HS, Graham DK. TAM receptor tyrosine kinases: biologic functions, signaling, and potential therapeutic targeting in human cancer. *Adv Cancer Res* 2008;100:35–83.
- Verma A, Warner SL, Vankayalapati H, Bearss DJ, Sharma S. Targeting AXL and Mer kinases in cancer. *Mol Cancer Ther* 2011;10:1763–73.
- Li Y, Ye X, Tan C, Hongo JA, Zha J, Liu J, et al. AXL as a potential therapeutic target in cancer: role of AXL in tumor growth, metastasis and angiogenesis. *Oncogene* 2009;28:3442–55.
- Linger RM, Keating AK, Earp HS, Graham DK. Taking aim at Mer and AXL receptor tyrosine kinases as novel therapeutic targets in solid tumors. *Expert Opin Ther Targets* 2010;14:1073–90.
- Paccez JD, Vogelsang M, Parker MI, Zerbini LF. The receptor tyrosine kinase AXL in cancer: biological functions and therapeutic implications. *Int J Cancer* 2014;134:1024–33.
- Zhang YX, Knyazev PG, Cheburkin YV, Sharma K, Knyazev YP, Orfi L, et al. AXL is a potential target for therapeutic intervention in breast cancer progression. *Cancer Res* 2008;68:1905–15.
- Rankin EB, Fuh KC, Taylor TE, Krieg AJ, Musser M, Yuan J, et al. AXL is an essential factor and therapeutic target for metastatic ovarian cancer. *Cancer Res* 2010;70:7570–9.
- Paccez JD, Vasques GJ, Correa RG, Vasconcellos JF, Duncan K, Gu X, et al. The receptor tyrosine kinase AXL is an essential regulator of prostate cancer proliferation and tumor growth and represents a new therapeutic target. *Oncogene* 2013;32:689–98.
- Liu R, Gong M, Li X, Zhou Y, Gao W, Tulpule A, et al. Induction, regulation, and biologic function of AXL receptor tyrosine kinase in Kaposi sarcoma. *Blood* 2010;116:297–305.
- Linger RM, Cohen RA, Cummings CT, Sather S, Migdall-Wilson J, Middleton DH, et al. Mer or AXL receptor tyrosine kinase inhibition promotes apoptosis, blocks growth and enhances chemosensitivity of human non-small cell lung cancer. *Oncogene* 2013;32:3420–31.
- Han J, Tian R, Yong B, Luo C, Tan P, Shen J, et al. Gas6/AXL mediates tumor cell apoptosis, migration and invasion and predicts the clinical outcome of osteosarcoma patients. *Biochem Biophys Res Commun* 2013;435:493–500.
- Byers LA, Diao L, Wang J, Saintigny P, Girard L, Peyton M, et al. An epithelial–mesenchymal transition gene signature predicts resistance to EGFR and PI3K inhibitors and identifies AXL as a therapeutic target for overcoming EGFR inhibitor resistance. *Clin Cancer Res* 2013;19:279–90.
- Giles KM, Kalinowski FC, Candy PA, Epis MR, Zhang PM, Redfern AD, et al. AXL mediates acquired resistance of head and neck cancer cells to the epidermal growth factor receptor inhibitor erlotinib. *Mol Cancer Ther* 2013;12:2541–58.
- Meyer AS, Miller MA, Gertler FB, Lauffenburger DA. The receptor AXL diversifies EGFR signaling and limits the response to EGFR-targeted inhibitors in triple-negative breast cancer cells. *Sci Signal* 2013;6:ra66.
- Ye X, Li Y, Stawicki S, Couto S, Eastham-Anderson J, Kallop D, et al. An anti-AXL monoclonal antibody attenuates xenograft tumor growth and enhances the effect of multiple anticancer therapies. *Oncogene* 2010;29:5254–64.
- Zhang Z, Lee JC, Lin L, Olivas V, Au V, LaFramboise T, et al. Activation of the AXL kinase causes resistance to EGFR-targeted therapy in lung cancer. *Nat Genet* 2012;44:852–60.
- Rho JK, Choi YJ, Kim SY, Kim TW, Choi EK, Yoon SJ, et al. MET and AXL inhibitor NPS-1034 exerts efficacy against lung cancer cells resistant to EGFR kinase inhibitors because of MET or AXL activation. *Cancer Res* 2014;74:253–62.
- Dunne PD, McCart DG, Blayney JK, Kalimutho M, Greer S, Wang T, et al. AXL is a key regulator of inherent and chemotherapy-induced invasion and predicts a poor clinical outcome in early-stage colon cancer. *Clin Cancer Res* 2014;20:164–75.
- Baselga J. The EGFR as a target for anticancer therapy—focus on cetuximab. *Eur J Cancer* 2001;37(Suppl 4):S16–22.
- Bonner JA, Harari PM, Giralt J, Azarnia N, Shin DM, Cohen RB, et al. Radiotherapy plus cetuximab for squamous-cell carcinoma of the head and neck. *N Engl J Med* 2006;354:567–78.
- Govindan R. Cetuximab in advanced non-small cell lung cancer. *Clin Cancer Res* 2004;10:4241S–4S.
- Pirker R, Pereira JR, Szczesna A, von Pawel J, Krzakowski M, Ramlau R, et al. Cetuximab plus chemotherapy in patients with advanced non-small-cell lung cancer (FLEX): an open-label randomised phase III trial. *Lancet* 2009;373:1525–31.
- Thienelt CD, Bunn PA, Hanna N, Rosenberg A, Needle MN, Long ME, et al. Multicenter phase I/II study of cetuximab with paclitaxel and carboplatin in untreated patients with stage IV non-small-cell lung cancer. *J Clin Oncol* 2005;23:8786–93.
- Van Cutsem E, Kohne CH, Hitre E, Zaluski J, Chang Chien CR, Makhson A, et al. Cetuximab and chemotherapy as initial treatment for metastatic colorectal cancer. *N Engl J Med* 2009;360:1408–17.
- Vermorken JB, Mesia R, Rivera F, Remenar E, Kawecki A, Rottey S, et al. Platinum-based chemotherapy plus cetuximab in head and neck cancer. *N Engl J Med* 2008;359:1116–27.
- Lynch TJ, Patel T, Dreisbach L, McCleod M, Heim WJ, Hermann RC, et al. Cetuximab and first-line taxane/carboplatin chemotherapy in advanced non-small-cell lung cancer: results of the randomized multicenter phase III trial BMS099. *J Clin Oncol* 2010;28:911–7.
- Bardelli A, Siena S. Molecular mechanisms of resistance to cetuximab and panitumumab in colorectal cancer. *J Clin Oncol* 2010;28:1254–61.
- Brand TM, Iida M, Wheeler DL. Molecular mechanisms of resistance to the EGFR monoclonal antibody cetuximab. *Cancer Biol Ther* 2011;11:777–92.
- Diaz LA Jr, Williams RT, Wu J, Kinde I, Hecht JR, Berlin J, et al. The molecular evolution of acquired resistance to targeted EGFR blockade in colorectal cancers. *Nature* 2012;486:537–40.
- Wheeler DL, Huang S, Kruser TJ, Nechrebecki MM, Armstrong EA, Benavente S, et al. Mechanisms of acquired resistance to cetuximab: role of HER (ErbB) family members. *Oncogene* 2008;27:3944–56.
- Iida M, Brand TM, Starr MM, Li C, Huppert EJ, Luthar N, et al. Sym004, a novel EGFR antibody mixture, can overcome acquired resistance to cetuximab. *Neoplasia* 2013;15:1196–206.
- Brand TM, Dunn EF, Iida M, Myers RA, Kostopoulos KT, Li C, et al. Erlotinib is a viable treatment for tumors with acquired resistance to cetuximab. *Cancer Biol Ther* 2011;12:436–46.
- Iida M, Brand TM, Campbell DA, Li C, Wheeler DL. Yes and Lyn play a role in nuclear translocation of the epidermal growth factor receptor. *Oncogene* 2013;32:759–67.
- Brand TM, Iida M, Luthar N, Wlekinski MJ, Starr MM, Wheeler DL. Mapping C-terminal transactivation domains of the nuclear HER family receptor tyrosine kinase HER3. *PLoS ONE* 2013;8:e71518.
- Li C, Brand TM, Iida M, Huang S, Armstrong EA, van der Kogel A, et al. Human epidermal growth factor receptor 3 (HER3) blockade with U3-1287/AMG888 enhances the efficacy of radiation therapy in lung and head and neck carcinoma. *Discov Med* 2013;16:79–92.
- Li C, Iida M, Dunn EF, Ghia AJ, Wheeler DL. Nuclear EGFR contributes to acquired resistance to cetuximab. *Oncogene* 2009;28:3801–13.

37. Yarden Y, Pines G. The ERBB network: at last, cancer therapy meets systems biology. *Nat Rev Cancer* 2012;12:553–63.
38. Mudduluru G, Leupold JH, Stroebel P, Allgayer H. PMA up-regulates the transcription of AXL by AP-1 transcription factor binding to TRE sequences via the MAPK cascade in leukaemia cells. *Biol Cell* 2010;103:21–33.
39. Holland SJ, Pan A, Franci C, Hu Y, Chang B, Li W, et al. R428, a selective small molecule inhibitor of AXL kinase, blocks tumor spread and prolongs survival in models of metastatic breast cancer. *Cancer Res* 2010;70:1544–54.
40. Montagut C, Dalmases A, Bellosillo B, Crespo M, Pairet S, Iglesias M, et al. Identification of a mutation in the extracellular domain of the Epidermal Growth Factor Receptor conferring cetuximab resistance in colorectal cancer. *Nat Med* 2012;18:221–3.
41. Hatakeyama H, Cheng HX, Wirth P, Counsell A, Marcrom SR, Wood CB, et al. Regulation of heparin-binding EGF-like growth factor by miR-212 and acquired cetuximab-resistance in head and neck squamous cell carcinoma. *PLoS ONE* 2010;5:e12702.
42. Bianco R, Rosa R, Damiano V, Daniele G, Gelardi T, Garofalo S, et al. Vascular endothelial growth factor receptor-1 contributes to resistance to anti-epidermal growth factor receptor drugs in human cancer cells. *Clin Cancer Res* 2008;14:5069–80.
43. Normanno N, Tejpar S, Morgillo F, De Luca A, Van Cutsem E, Ciardiello F. Implications for KRAS status and EGFR-targeted therapies in metastatic CRC. *Nat Rev Clin Oncol* 2009;6:519–27.
44. Wheeler DL, Iida M, Kruser TJ, Nechrebecki MM, Dunn EF, Armstrong EA, et al. Epidermal growth factor receptor cooperates with Src family kinases in acquired resistance to cetuximab. *Cancer Biol Ther* 2009;8:696–703.
45. Siolas D, Hannon GJ. Patient-derived tumor xenografts: transforming clinical samples into mouse models. *Cancer Res* 2013;73:5315–9.
46. Kimple RJ, Harari PM, Torres AD, Yang RZ, Soriano BJ, Yu M, et al. Development and characterization of HPV-positive and HPV-negative head and neck squamous cell carcinoma tumorgrafts. *Clin Cancer Res* 2013;19:855–64.
47. Zhang L, Castanaro C, Luan B, Yang K, Fan L, Fairhurst JL, et al. ERBB3/HER2 signaling promotes resistance to EGFR blockade in head and neck and colorectal cancer models. *Mol Cancer Ther* 2014;13:1345–55.